

Human Social Cycling Spectrum

Wang Zhijian and Yao Qinmei

Experimental Social Science Laboratory,
Zhejiang University, Hangzhou 310058, China

June 18, 2021

This paper investigates the reality and accuracy of evolutionary game dynamics theory in human game behavior experiments. In classical game theory, the central concept is Nash equilibrium, which reality and accuracy has been well known since the firstly illustration by the O'Neill game experiment in 1987. In game dynamics theory, the central approach is dynamics equations, however, its reality and accuracy is rare known, especially in high dimensional games. By develop a new approach, namely the eigencycles approach, with the eigenvectors from the game dynamics equations, we discover the high dimensional cycles in the same experiments. We show that, the eigencycle approach can increase the accuracy by an order of magnitude in data. As the eigenvector is fundamental in dynamical systems theory which has applications in natural, social, and virtual worlds, the power of the eigencycles is expectedly. Inspired by the eigencycles in O'Neill games, we suggest that, the mathematical concept, namely 'invariant manifolds', can be a candidate as the central concept for the game dynamics theory, like the fixed point concept (Nash equilibrium) in game statics theory.

Keywords:

behavior game experiment
evolutionary game theory
dynamics system theory
eigenvector component
eigencycle
invariant manifold

Contents

1	Introduction	3
1.1	Research question	3
1.2	Background of eigencycle approach	3
1.3	Contents organization	4
2	Theoretical results on the eigencycle set	4
2.1	The eigenvector in the O'Neill game	4
2.2	Eigencycle set	5
2.3	Explanation of the theoretical results	6
3	Experimental observation on subspace cycles	8
3.1	Brief summary of the experiment data	8
3.2	Angular momentum as the measurement	8
3.3	Experimental results	9
3.4	Explanation of the experimental results:	9
4	Eigencycle set verified with experiments	11
4.1	Fine structure	11
4.2	Hyperfine structure	13
4.3	Eigencycle spectrum analysis	15
5	Discussion and conclusion	16
6	Appendix	19
6.1	Appendix 1: Geometrical interpretation of eigencycle	19
6.2	Appendix 2: Invariant between eigencycle and the angular momentum	20
6.2.1	Interfere of two components from the same eigenvector	20
6.2.2	Interfere of two components from two different eigenvector	21
6.3	Appendix 4: The eigen system derivation and symmetry analysis	23
6.3.1	The eigen system derivation	23
6.3.2	Eigen system and invariant manifold	24
6.3.3	The Lissajous figure and its statistics meaning	25
6.3.4	The eigen system symmetry	25
6.4	Appendix 6: Verification of the invariant manifold and eigencycle	25
6.5	Appendix 7: Verification of the net transit and eigencycle	27
6.6	Appendix 5: Data and dynamics model valid	28
6.7	Appendix 3: Related works	30
6.7.1	Related works on the evolutionary game theory and experiment	30
6.7.2	Related works on the dynamics system theory	31
6.7.3	Related works on the dynamics cycle in O'Neill game	32
6.7.4	Related work on high dimension game dynamics pattern	32

1 Introduction

1.1 Research question

We investigate the reality and accuracy of evolutionary game dynamics theory [20][9] in high dimensional human game behavior experiments [5].

In game statics theory, the mixed strategy Nash equilibrium established around 1950 is the central concept. Until 1987, a representative game experiment, the O'Neill game[18], provided the first illustration that laboratory human strategy behavior can be accurately captured by the central concept. Table 1 shows the payoff matrix of the experiments involving a long-run repeated, discrete time, two-person, zero-sum game. Since then, this game has been extensively repeated in various experimental settings [15][17] and analysis [3]. So far, the literature has focused on the long time strategy distributions and the time dependence of individual behaviors, but seldom explored social dynamics structure. Here, the dynamics structure means the geometrical pattern of the evolutionary trajectories in the game state space.

Intuitively, two reasons hinder the study of the dynamics pattern. First, the game has a high-dimension strategy space; the means to handle the high dimensional dynamic pattern remains an unresolved problem [7]. Second, in a laboratory game experiment, human strategy decision-making is highly stochastic, and testing the dynamic pattern is a difficult task [5][14], especially in a discrete time game [6]. Past decade has seen the improvement on test out cyclic dynamical pattern in some presentative games, like rock-paper-scissors [6, 24] and matching pennies-like 2×2 game [25]. But actually, all of these are two dimensional, not high dimensional. In a real game, there always many players and many strategy involve, then the evolution trajectory will be in high dimensional state space.

To study high dimension game dynamics structure is not trivial. As a cutting-edge question, not only in laboratory game experiments, it appears in seeking the regularity in real game dynamics processes. It is meaningful for the natural science and social science, as well as in engineering and artificial intelligent visual world [9][20][7]. One can say that, in a real or visual world, wherever the game theory can be applied, during game playing, there always exists evolutionary processes; Then in the processes which appearing as geometrical trajectories, the regularity always a curious question.

1.2 Background of eigencycle approach

We thus develop an approach, the **eigencycle set** to identify the high dimensional dynamics. Our approach bases on dynamical systems theory, a branch of mathematics. As established before, for the local dynamics near the equilibrium, the linearization and analytical solutions based on the eigenvalues and eigenvectors can be applied. Suppose that an initial probability distribution can be expressed as a linear combination of the eigenvectors ξ as [16],

$$p(0) = a_1\xi_1 + a_2\xi_2 + \dots + a_k\xi_k, \quad (1)$$

wherein ξ_i is associated eigenvector of the eigenvalue λ_i ; The probability will evolve in time according to

$$p(t) = e^{\lambda_1 t} a_1 \xi_1 + e^{\lambda_2 t} a_2 \xi_2 + \dots + e^{\lambda_k t} a_k \xi_k, \quad (2)$$

where, the coefficients $(a_i, i \in [1, k])$ and $(\xi_i, i \in [1, k])$ are independent of time t , and the only time depending term is $e^{\lambda_i t}$. Instead of the coefficients a_i or the eigenvalue λ_i , we concern the components of the eigenvectors. Suppose a normalized eigenvector having s components and denoting as $\xi_i = (\eta_1, \dots, \eta_m, \dots, \eta_n, \dots, \eta_s)$, we can present the m -th dimension evolution as

$$p_m(t) = e^{\lambda_1 t} a_1 \eta_{m1} + e^{\lambda_2 t} a_2 \eta_{m2} + \dots + e^{\lambda_k t} a_k \eta_{mk}. \quad (3)$$

Similarily, the n -th dimension evolution as

$$p_n(t) = e^{\lambda_1 t} a_1 \eta_{n1} + e^{\lambda_2 t} a_2 \eta_{n2} + \dots + e^{\lambda_k t} a_k \eta_{nk}. \quad (4)$$

Obviously, $p_m(t)$ and $p_n(t)$ will form a trajectory in the two dimensional space (hereafter denoted as Ω^{mn} which is a subspace of the s dimensional space).

Our starting point comes from the synchronization between two components belong to a given eigenvector. There exists two time invariant: First, the phase angle difference of any two components $(\arg(\eta_m) - \arg(\eta_n))$ is invariant along time; Second, the amplitude of each component η_i , $||\eta_i||$, is

invariant along time. Then we study the inference of two components in general conditions. By which, we develop a new theoretical expected observation, called as eigencycle set, to identify human dynamics behaviors in a high-dimensional game.

The main contributions are as follows: (1) As illustrated in Figure 2, we find the fine and hyperfine structures in high-dimensional game dynamics pattern in a historic human game experiment data, with the cycle measurement accuracy increased by an order of magnitude. (2) We propose a tool, the eigencycle set analysis, for general dynamics system analysis. We illustrate its validation in the O' Neill game data who firstly illustrated the accuracy of Nash equilibrium in 1987.

Inspired by the finding in experiments as well as the approach which deeply rooted in standard dynamics system theory, we suggest that, the central concept of game dynamics theory needs to be reconsidered, which will be discussed later.

1.3 Contents organization

The rest of this paper is organized as follows: In section 2, we introduce the O'Neill game as the example, and analytical calculate the eigen system of the replicator dynamics equations; Then we illustrate the eigencycle set approach and the theoretical results, from which the fine structure and hypofine structure are predicted; In section 3, we introduce the six human behavior game experiment data, and report the experimental results of the high dimensional cycle motion projection on the two dimensional subspaces; In section 4, we validate the theoretical eigencycle set approach for bridging theory and experiments. In this section, the discovery of the fine structure and the significant evidence of the hyperfine structure are reported. In section 5, we summarize our contributions, the implication of our finding and the approach and present the scope for future research. At the last, by numerical results comparisons, we suggest that, the 'invariant manifold' can be the potential central concept for game dynamics theory.

2 Theoretical results on the eigencycle set

2.1 The eigenvector in the O'Neill game

The O'Neill game is a zero-sum, 4×4 game. Table 1 shows the payoff matrix: To investigate dynamics

Table 1: The O'Neill zero-sum game matrix

	B1	B2	B3	B4
A1	1	-1	-1	-1
A2	-1	-1	1	1
A3	-1	1	-1	1
A4	-1	1	1	-1

behavior in a laboratory experiment game, we use the replicator dynamics equation [20]:

$$\dot{x}_j = x_j * (U_j - \overline{U_X}), \quad (5)$$

x_j is the j th strategy player's probability in the population with the j th strategy player included, and \dot{x}_j is the evolution velocity of the probability; U_j the payoff of the j th strategy player, and $\overline{U_X}$ is the average payoff of the population with the j th strategy player included. The explicitly expression of these nonlinear differential equations are shown in SI.

One by one, we assign strategy probabilities (A1, A2, A3, A4) to (x_1, x_2, x_3, x_4) , respectively. Similarly, we assign strategy probabilities (B1, B2, B3, B4) to (x_5, x_6, x_7, x_8) , respectively. Then, at any time, the system must be an eight-dimension space, wherein the Nash equilibrium is

$$x^* := (x_1^*, x_2^*, \dots, x_8^*) = (2/5, 1/5, 1/5, 1/5, 2/5, 1/5, 1/5, 1/5).$$

This eight-dimension space has two concentrated

$$x_1 + x_2 + x_3 + x_4 = 1 \cap x_5 + x_6 + x_7 + x_8 = 1 \cap x_k \geq 0 \quad (k \in 1, 2, \dots, 8)$$

From the Jacobian matrix (or character matrix, or derivative matrix) of the velocity vector field $F := (\dot{x}_1, \dot{x}_2, \dots, \dot{x}_8)$ at Nash equilibrium x^* [20], we can calculate the eigenvalues λ and their related normalized eigenvector ξ 's components $(\eta_1, \eta_2, \dots, \eta_8)$ explicitly. Here, the components $(\eta_1, \eta_2, \dots, \eta_8)$ are one-by-one corresponding to (x_1, x_2, \dots, x_8) . The explicitly analytic results of the eigenvalue λ and eigenvector ξ are shown in Table 2. From the sign of the eigenvalues we can read off that the Nash equilibrium (fixed point) is linearly along the eigendirection of the real eigenvalues. Details of the eigen system deduction are shown in appendix section 6.3.

2.2 Eigencycle set

Definition

We call the circle constructed by the two components (η_m, η_n) within one normalized eigenvector $\xi_i = (\eta_1, \dots, \eta_m, \dots, \eta_n, \dots, \eta_s)$ the **eigencycle**, marked as $\sigma^{(mn)}$. It is calculated as:

$$\sigma^{(mn)} = \pi \cdot \|\eta_m\| \cdot \|\eta_n\| \cdot \sin(\arg(\eta_m) - \arg(\eta_n)), \quad (6)$$

where m and n are the abscissa and the ordinate dimension of the two dimension subspace, respectively. $\|\eta_m\|$ and $\arg(\eta_m)$ indicate the amplitude and the phase angle of the η_m , respectively. $\sigma^{(mn)}$ can determine the direction and amplitude of the eigencycle. An alternative and equivalent presentations of the eigencycle value are

$$\sigma^{(mn)} = \pi \cdot (\Re(\eta_m)\Im(\eta_n) - \Re(\eta_n)\Im(\eta_m)), \quad (7)$$

$$= \pi \cdot \Re(\eta_m^\dagger \eta_n) \quad (8)$$

wherein the $\Re(\eta_m)$ is the real part of the complex number η_m and the $\Im(\eta_m)$ is the imaginary part; the superscript \dagger indicates the conjugate of the complex number.

Eigencycle values of the O'Neill game

According to this formula, for the O'Neill game, Table 2 lists the eigencycle values of the eigenvectors of the replicator dynamics.

Interpretation of the definition

- **Invariance of the eigencycle:** An eigencycle is constructed by two components in a normalized eigenvector, and hence, its value is invariant. This is according to Eq. (7) and the following points: (1) the mode of each component is fixed; and (2) the phase difference between two given components in an eigenvector is fixed; Because, they are modulated by the same eigenvalue, that is, the relative phase difference between these two components remains fixed.
- **Number of eigencycle:** There are $N(N-1)/2$ independent eigencycles corresponding to a given N -component normalized eigenvector, as there are N^2 pairwise combinations of each component in an N -dimensional eigenvector. Considering that the N self-combination of (η_m, η_m) is trivial ($\sigma^{(mm)} = 0$), and (η_n, η_m) and (η_m, η_n) are simply reversed ($\sigma^{(mn)} = -\sigma^{(nm)}$), only $N(N-1)/2$ combinations remain.
- **Eigencycle set:** The eigencycle set, as a vector denoted by $\Omega_{\xi_k}^{(mn)}$, is defined to represent a set of $N(N-1)/2$ eigencycle elements. The subscript is the normalized eigenvector ξ indexed by k , which generates this eigencycle set. The superscript (mn) is the index of the two-dimensional subspace, where the elements (eigencycles) of the set are located. (mn) is defined as follows: $\{\{m, n\} \in \{1, 2, \dots, n\} \cap (m < n)\}$. In this study, the assignment order is m from 1 to N , and then n from 2 to N .
- **Subspace set:** The subspace set, denoted as $\Omega^{(mn)}$, has $N(N-1)/2$ eigencycle elements. The superscript (mn) is the index of the two-dimensional subspace. Again, (mn) is defined as follows: $\{\{m, n\} \in \{1, 2, \dots, n\} \cap (m < n)\}$. In this study, the assignment order is m from 1 to N , and then n from 2 to N . Owing to symmetry, there exists a subset of $\Omega^{(mn)}$, wherein the performance of the elements is equal.

- **Independence of eigencycle sets:** The eigencycle sets corresponding to eigenvectors are not all independent. Let us take the O'Neill game as an example. Among the eight eigencycle sets, only three (generated by $(\xi_{.8i}, \xi_{.4i_1}, \xi_{.4i_2})$) are independent. We explain this as follows: Per the set of eigenvalues, (1) Two eigenvalues (0.2 and -0.2) are real numbers. As only the eigenvectors whose eigenvalues are complex numbers are related to cyclical motion, these two are trivial. (2) The remaining six eigenvectors make three pairs. Each pair of eigenvectors with complex conjugate eigenvalues are conjugate, and the generated eigencycle set pair has opposite values to the other pair. Hence, we can omit those related to eigenvalues, that is, $(-0.8i, -0.4i, -0.4i)$. Using the eigenvalues as the subscript symbols, the eigenvectors are recorded as $(\xi_{.8i}, \xi_{.4i_1}, \xi_{.4i_2})$. In this system, there two independent eigenvectors (5-th and 7-th in Table 2) belong to the same eigenvalue $-0.4i$. We use the subscripts 1 and 2 to distinguish the eigencycle set from the two degenerate eigenvalues of $0.4i$.
- **Geometric presentation:** A geometric presentation of an eigencycle set is shown in figure 1. An eigencycle only depends on the internal components η_m and η_n of the same normalized eigenvector. As both of the components' amplitude and phase difference is fixed and not arbitrary, so the geometric pattern set is fixed. In geometry, an elements of the eigencycle set is similar to a Lissajous cycle. An explanation of the similarity is shown in appendix section 6.1.
- **Relationship between eigencycle value and angular momentum:** In mathematics, we can strictly prove that, the rate between the angular momentum at any time moment in any two subspace equals to the rate between eigencycle values of the two subspace. See appendix section 6.2 for details. Meanwhile, in a time series from a real experiment system, the angular momentum of the two observations in time series is measurable. So the eigencycle concept can be verified in real system.
- **Why the O'Neill game?** Since O'Neill is a two-person four-strategy zero-sum game with eight dimensions, it is a high-dimensional problem. It is difficult for us to intuitively express the motion structure of such a high dimension. Using the eigencycle set, the eight-dimension game space can be decomposed into 28 two-dimension sets. Importantly,
 - In theory, this game's replicator dynamics equation can be explicitly solved mathematically. The game has high symmetry, so it is easily tractable.
 - In experiment, the game matrix has high symmetry and there exist sufficient equivalent observations. The data should provide sufficient opportunity for testing.
 - The O'Neill experiment was the first to reveal the reality and accuracy of the Nash Equilibrium in game theory. Revealing these characteristics of game dynamics using our experiment data is a new challenge.

2.3 Explanation of the theoretical results

Here, we briefly explain the theoretical results in Table 2. Meanwhile, define the fine structure and hypfine structure in the O'Neil game.

- **Precision and fine structure** Table 2 provides a theoretical prediction on cyclic behavior having higher precision than ever known. The eigencycle set $\sigma_{.8i}$ predicts four different values, $(0.1964:0.0654:0.0218:0) = (9:3:1:0)$, that is, a cycle set with four different strengths are expected. This prediction leads to (1) the discovery of the fine structure (see section 4.1); (2) the rising of the test accuracy one order (see section 3.4), which are included in the main results of this study.
- **Symmetry and hypfine structure** The contributions of the eigencycles from the different normalized eigenvectors ξ are different, but can be classified as shown in the numerical results in Table 2. The classification reflects the symmetry of the game matrix as well as the structure of the ξ inner components. We employ this to identify the contribution of ξ in the data (e.g., see σ_α and σ_β in subsection 4.2), which is one of the main results of this study too.
- **Operable** — We use the experiment data to validate our eigencycle set decomposition approach. Our results may provide a spectrum analysis tool for game dynamics (see section 4.3).

Table 2: The eigenvalues, eigenvectors, and their respective 28 eigencycles

Eigenvalue λ_i	$\lambda_{.8i}$	$\lambda_{-.8i}$	$\lambda_{.2}$	$\lambda_{-.2}$	$\lambda_{.4i_1}$	$\lambda_{-.4i_1}$	$\lambda_{.4i_2}$	$\lambda_{-.4i_2}$
	$\frac{4}{5}i$	$-\frac{4}{5}i$	$\frac{1}{5}$	$-\frac{1}{5}$	$\frac{2}{5}i_1$	$-\frac{2}{5}i_1$	$\frac{2}{5}i_2$	$-\frac{2}{5}i_2$
Eigenvector ($\eta_i \in \xi$)	$\xi_{.8i}$	$\xi_{-.8i}$	$\xi_{.2}$	$\xi_{-.2}$	$\xi_{.4i_1}$	$\xi_{-.4i_1}$	$\xi_{.4i_2}$	$\xi_{-.4i_2}$
η_1	$-\frac{1}{4}i$	$\frac{1}{4}i$	$\frac{2}{5}$	0	0	0	0	0
η_2	$\frac{1}{12}i$	$-\frac{1}{12}i$	$\frac{1}{5}$	0	$\frac{1}{6}$	$\frac{1}{6}$	$\frac{1}{6}$	$\frac{1}{6}$
η_3	$\frac{1}{12}i$	$-\frac{1}{12}i$	$\frac{1}{5}$	0	$\frac{-1+\sqrt{3}i}{12}$	$\frac{-1-\sqrt{3}i}{12}$	$\frac{-1-\sqrt{3}i}{12}$	$\frac{-1+\sqrt{3}i}{12}$
η_4	$\frac{1}{12}i$	$-\frac{1}{12}i$	$\frac{1}{5}$	0	$\frac{-1-\sqrt{3}i}{12}$	$\frac{-1+\sqrt{3}i}{12}$	$\frac{-1+\sqrt{3}i}{12}$	$\frac{-1-\sqrt{3}i}{12}$
η_5	$\frac{1}{4}i$	$-\frac{1}{4}i$	0	$\frac{2}{5}$	0	0	0	0
η_6	$-\frac{1}{12}$	$-\frac{1}{12}$	0	$\frac{1}{5}$	$-\frac{i}{6}$	$\frac{i}{6}$	$-\frac{i}{6}$	$\frac{i}{6}$
η_7	$-\frac{1}{12}$	$-\frac{1}{12}$	0	$\frac{1}{5}$	$\frac{\sqrt{3}+i}{12}$	$\frac{\sqrt{3}-i}{12}$	$\frac{-\sqrt{3}+i}{12}$	$\frac{-\sqrt{3}-i}{12}$
η_8	$-\frac{1}{12}$	$-\frac{1}{12}$	0	$\frac{1}{5}$	$\frac{-\sqrt{3}+i}{12}$	$\frac{-\sqrt{3}-i}{12}$	$\frac{\sqrt{3}+i}{12}$	$\frac{\sqrt{3}-i}{12}$
Eigencycle ($\Omega^{(mn)}$)	$\sigma_{.8i}$	$\sigma_{-.8i}$	$\sigma_{.2}$	$\sigma_{-.2}$	$\sigma_{.4i_1}$	$\sigma_{-.4i_1}$	$\sigma_{.4i_2}$	$\sigma_{-.4i_2}$
12	0	0	0	0	0	0	0	0
13	0	0	0	0	0	0	0	0
14	0	0	0	0	0	0	0	0
15	-0.1964	0.1964	0	0	0	0	0	0
16	0.0654	-0.0654	0	0	0	0	0	0
17	0.0654	-0.0654	0	0	0	0	0	0
18	0.0654	-0.0654	0	0	0	0	0	0
23	0	0	0	0	-0.0756	0.0756	0.0756	-0.0756
24	0	0	0	0	0.0756	-0.0756	-0.0756	0.0756
25	0.0654	-0.0654	0	0	0	0	0	0
26	-0.0218	0.0218	0	0	0.0873	-0.0873	0.0873	-0.0873
27	-0.0218	0.0218	0	0	-0.0436	0.0436	-0.0436	0.0436
28	-0.0218	0.0218	0	0	-0.0436	0.0436	-0.0436	0.0436
34	0	0	0	0	-0.0756	0.0756	0.0756	-0.0756
35	0.0654	-0.0654	0	0	0	0	0	0
36	-0.0218	0.0218	0	0	-0.0436	0.0436	-0.0436	0.0436
37	-0.0218	0.0218	0	0	0.0873	-0.0873	0.0873	-0.0873
38	-0.0218	0.0218	0	0	-0.0436	0.0436	-0.0436	0.0436
45	0.0654	-0.0654	0	0	0	0	0	0
46	-0.0218	0.0218	0	0	-0.0436	0.0436	-0.0436	0.0436
47	-0.0218	0.0218	0	0	-0.0436	0.0436	-0.0436	0.0436
48	-0.0218	0.0218	0	0	0.0873	-0.0873	0.0873	-0.0873
56	0	0	0	0	0	0	0	0
57	0	0	0	0	0	0	0	0
58	0	0	0	0	0	0	0	0
67	0	0	0	0	-0.0756	0.0756	0.0756	-0.0756
68	0	0	0	0	0.0756	-0.0756	-0.0756	0.0756
78	0	0	0	0	-0.0756	0.0756	0.0756	-0.0756

Note: $\Omega^{(mn)}$ is the identity of the two-dimensional subspace of an eigencycle. m (n) indicates which among the eight dimensions is selected as the x -axis (y -axis) in the eigencycle subspace.

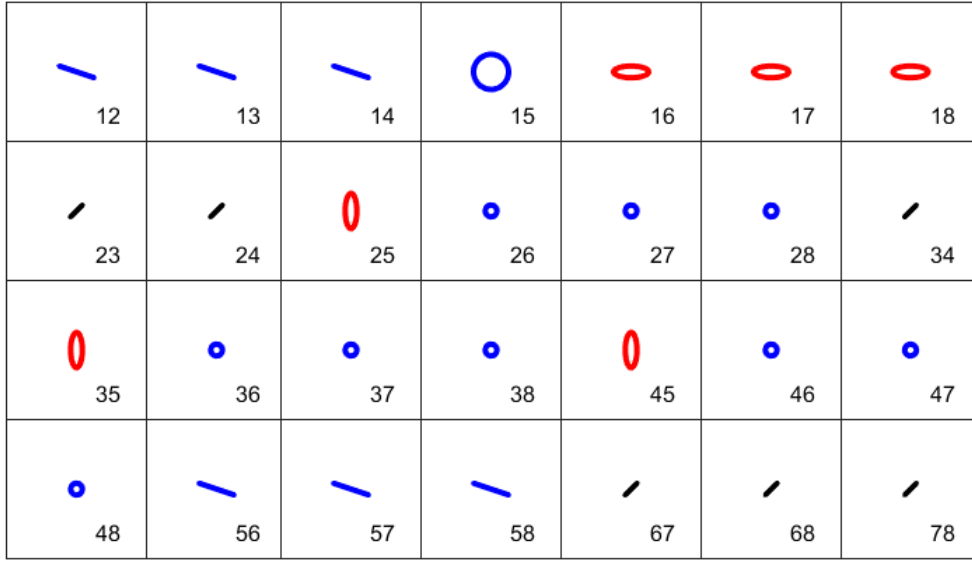


Figure 1: Geometric presentation of the eigencycle set. Subfig (mn) illustrate the 28 eigencycles patterns of the eigencycle set ($\sigma_{.8i}$); the value of eigenvector component (η_m and η_n) and cycles value $\Omega^{(mn)}$ is shown in Table 2. The red (blue) color indicates the cyclic motion being counter-clockwise (clockwise), and its value (called as the signed area value or the angular momentum value), is positive (negative).

3 Experimental observation on subspace cycles

3.1 Brief summary of the experiment data

Table 3 summarizes the O'Neill game experiments. The three experiments span 26 years. In total, 358 subjects participated in the experiments, which involved multi-round repeated playing in the game matrix 1. The experiment data help verify the high-dimensional cycling in this study.

Table 3: Experiment Data Source

Experiment abbreviate	Data Source	Experiment Summary	Published Time	total Rounds	Matching Protocol
<i>O</i>	O'Neill	The game was played by 50 students working in 25 pairs.	1987	2625	Fixed Paired
<i>B</i>	Binmore et al	Each experiment session required 12 subjects 13 experimental sessions in all. Each real game was played 150 times.	2001	1950	Randomly Matching
<i>IT</i>	Okano	20 individuals adopted the player A role against 20 teams adopting the player B role. 20 experimental sessions in all. Each real game was played 150 times.	2013	3000	Fixed Paired
<i>TI</i>	Okano	20 teams adopted the player A role against 20 individuals adopting the player B role, 20 experimental sessions in all. Each real game was played 150 times.	2013	3000	Fixed Paired
<i>II</i>	Okano	Individuals against individuals, 18 experimental sessions in all. Each real game was played 132 times.	2013	2376	Fixed Paired
<i>TT</i>	Okano	Teams against teams, 18 experimental sessions in all. Each real game was played 132 times.	2013	2376	Fixed Paired

3.2 Angular momentum as the measurement

The measurement for the cycle in the subspace:

According to the theoretical eigencycle set decomposition approach, we can measure the cyclic angular momentum ¹ in each of the two-dimensional subspace, indicated by the eigencycle $\Omega^{(mn)}$, separately. The angular momentum $L_E^{(mn)}$ [27] can be expressed by the following formula:

$$L_E^{mn} = \frac{1}{N-1} \sum_{t=1}^{N-1} (x(t) - O) \times (x(t+1) - x(t)) \quad (9)$$

- $L_E^{(mn)}$ represents the average value of the accumulated angular momentum over time; the subscript mn indexes the two-dimensional (x_m, x_n) subspace;
- N is the length of the experimental time series, that is, the total number of repetitions of the repeated game experiments;
- O is the projection of the Nash equilibrium at the subspace $\Omega^{(m,n)}$;
- $x(t)$ is a two-dimensional vector at time t , which can be expressed as $(x_m(t), x_n(t))$, $x(t+1)$ is a two-dimensional vector at time $t+1$, and
- \times represents the cross product between two two-dimensional vectors.

Interpretation of the measurement:

- The sign of the value of $L_E^{(mn)}$ indicates the direction of the cyclical movement (counterclockwise or clockwise): $L_E^{(mn)} > 0$ refers to counterclockwise movement and $L_E^{(mn)} < 0$ refers to clockwise movement. $L_E^{(mn)} = 0$ means no cycle was observed. If a system is completely random, as predicted by the mixed strategy Nash equilibrium, the long-term average of its angular momentum is 0.
- The modulus of the value, $\|L_E^{(mn)}\|$, indicates the strength of determinate motion. For example, in a one-to-one fixed pairing, there are four states in a two-dimensional subspace, and these four states form a unit square with an area of 1. The accumulated angular momentum of one full cycle is 2, or $\|L_E^{(mn)}\| = 2$.
- If, in the time series of 1,000 repeated rounds experiment, the observed accumulated $L_E^{(mn)} = 40$, then the total amount of the determinate motion is 20 cycles. This also means there are 80 determinate motions beyond complete stochastic motion, that is, the probability of directional movement is 8%.

3.3 Experimental results

We calculate the average angular momentum for the experiments shown in Table 3, and Table 4 shows the results.

3.4 Explanation of the experimental results:

The measurement results illustrate the consistency and precision of the six experiments, thus validating the inner eigenvector decomposition approach. The cycles in the high-dimension space are real and testable as well, as shown by the following two points:

- **Consistency** — In the six experiments, the observed cycle values L in the two-dimensional subspaces show consistency (Spearman rank's test, $\max(p)=0.012$, mean of the ρ values is 0.6351, Std. Ev = 0.1087, Std. Err = 0.0118).
- **Precision** — Except for the main cycle found in $\Omega^{(15)}$, we can now test the cycles in the subspace ($\Omega^{(26,27,28,36,37,38,46,47,48)}$). This means that the accuracy increases up to one order of magnitude. We explain this with two numerical examples:

¹This measurement is the signed area of the triangle $\Delta_{[O,x(t),x(t+1)]}$ in the (m,n) two-dimensional subspace. For each transition from $x(t)$ to $x(t+1)$, referring to O , the angular momentum is twice the signed area of the triangle. We suggest using the angular momentum because it contains the mass m as a parameter, which may be compatible with the population size N as the variable in further investigations of game dynamics.

Table 4: Experimental angular momentum

$\Omega^{(mn)}$	$L_O^{(mn)}$	$L_B^{(mn)}$	$L_{IT}^{(mn)}$	$L_{TI}^{(mn)}$	$L_{II}^{(mn)}$	$L_{TT}^{(mn)}$
12	0.003	0.002	-0.008	-0.001	0.002	0.008
13	-0.011	-0.002	0.003	0.000	-0.009	-0.002
14	0.008	0.000	0.004	0.002	0.007	-0.006
15	-0.038	-0.015	-0.053	-0.033	-0.039	-0.049
16	0.009	0.010	0.018	0.019	0.008	0.020
17	0.021	0.002	0.020	0.006	0.015	0.014
18	0.007	0.003	0.015	0.008	0.016	0.014
23	0.011	0.003	-0.009	0.001	0.008	0.007
24	-0.008	-0.001	0.001	-0.002	-0.006	0.001
25	0.010	0.003	0.021	0.005	0.015	0.018
26	-0.001	0.000	0.004	-0.011	0.002	-0.009
27	-0.001	-0.001	-0.010	0.004	-0.012	-0.014
28	-0.007	-0.002	-0.014	0.002	-0.005	0.005
34	0.000	0.001	-0.006	0.000	-0.001	0.005
35	0.011	0.008	0.015	0.011	0.014	0.013
36	-0.009	-0.006	-0.003	-0.002	-0.006	-0.005
37	-0.003	0.001	-0.004	-0.004	0.002	0.002
38	0.002	-0.002	-0.008	-0.006	-0.011	-0.010
45	0.018	0.004	0.017	0.017	0.010	0.019
46	0.000	-0.004	-0.019	-0.006	-0.003	-0.007
47	-0.016	-0.001	-0.006	-0.007	-0.006	-0.002
48	-0.002	0.002	0.007	-0.004	-0.001	-0.009
56	-0.006	0.001	-0.001	0.001	-0.001	0.002
57	0.009	0.000	0.004	0.005	-0.005	-0.009
58	-0.003	-0.001	-0.002	-0.006	0.006	0.007
67	-0.003	0.001	-0.003	0.000	0.005	0.007
68	-0.003	0.000	0.002	0.001	-0.006	-0.005
78	0.006	0.000	0.000	0.005	0.000	-0.002

$\Omega^{(mn)}$ is the 28 subspaces referring to Table 2; the subscript L refers to the O'Neill and Binmore as well as the AIBT, ATBI, AIBI, and ATBT experiments in Table 3. We use the software MATLAB, version R2018a.

Table 5: Consistency of the six experiments

	L_O	L_B	L_{IT}	L_{TI}	L_{II}	L_{TT}
L_O	1.000 0.000					
L_B	0.706 0.000	1.000 0.000				
L_{IT}	0.522 0.004	0.639 0.000	1.000 0.000			
L_{TI}	0.660 0.000	0.658 0.000	0.586 0.001	1.000 0.000		
L_{II}	0.728 0.000	0.825 0.000	0.608 0.001	0.5306 0.0037	1.000 0.000	
L_{TT}	0.474 0.011	0.756 0.000	0.470 0.012	0.5932 0.0009	0.770 0.000	1.000 0.000

Measure: Spearman's rank correlation. The number of observations is 28. The variables (observations) are the experimental angular momentum shown in Table 4. The first row reports the correlation coefficients, and the second row reports the significance level p . We use the software Stata, version:SE 15.1.

- $L_O^{(15)} = -0.038$, where the superscript O indicates the O’Neill game, superscript (15) indicates that the subspace measured is $\Omega^{(15)}$, and the negative sign means the cycle is clockwise. $\|L\| = 0.038$, that is, there are $(\frac{105 \times 0.038}{2} \simeq 2)$ two cycles obtained in the O’Neill (1987) 105-rounds game, and, in the 25 groups, 2,625 rounds of observations, yielding 50 cycles.
- $L_O^{(37)} = -0.003$, that is, the average angular momentum in subspace 37 is 0.003. Each complete cyclical motion in the four-states subspace of the O’Neill game contributes two units of angular momentum; then, the 105 rounds have 0.2 cycles, and the 2,625 rounds have 4.4 cycles.

4 Eigencycle set verified with experiments

We have shown the theoretical eigencycle values $\sigma^{(mn)}$ in Table. 2 and the experimental average angular momentum L_{mn} in Table 9.

There is following proposition — For various subspace (m, n) , the average accumulated angular momentum L_{mn} divided by its $\sigma^{(mn)}$ is invariant (Details of the mathematical proof is provided in appendix 6.2). That is to say, by take $\sigma^{(mn)}$ as predictor (independent variable) and take L_{mn} as the observation (dependent variables), a linear relation with truncation term being 0 can be expected. So, we can evaluate the validity of the eigencycle with the experimental L (average angular momentum).

The three subsections can be abstracted as follows:

1. Report the discovery of the fine structure, because of the contribution of $\sigma_{.8i}$ which is labeled as $0.8i$ in Figure 2;
2. Report the finding of the hyperfine structure, because of the contribution of $\sigma_{.4i_1}$ and $\sigma_{.4i_2}$ which is labeled as α and β in Figure 2, respectively;
3. Report the multi-OLE results (see Table 8) illustrate that the eigencycle set is an ideal basis in this study. The results validate the eigenvector set as a spectrum analysis tool on dynamics system.

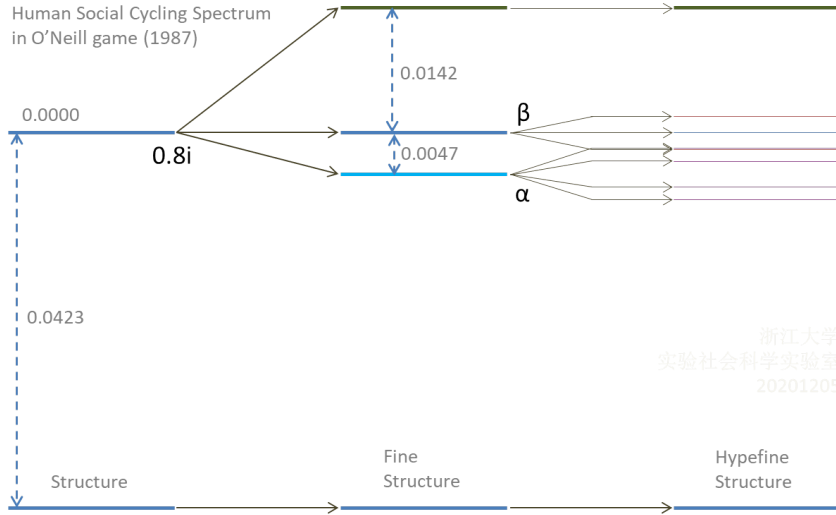


Figure 2: Fine and hyperfine structures of game dynamics in the O’Neill (1987) game experiments. The labels $\{0.0423, 0.0142, \text{ and } 0.047\}$ are the observed average angular momentum of the experiments, which linearly match the eigencycle values of $\sigma_{.8i}$. This figure illustrates how the theoretical eigencycle set clearly shows the existence of the the fine and hyperfine structures, thus enhancing the literature [15, 23, 6, 7].

4.1 Fine structure

Result 1’s description:

Table 6: Ordinary least squares between the six experimental L and $\{\sigma_{.8i}, \sigma_{.4i_1}, \sigma_{.4i_2}\}$

		$L_O^{(mn)}$	$L_B^{(mn)}$	$L_{IT}^{(mn)}$	$L_{TI}^{(mn)}$	$L_{II}^{(mn)}$	$L_{TT}^{(mn)}$
$\sigma_{.8i}$	coef. t	8.26	9.31	12.78	10.72	10.64	12.39
	p	(0.00)	(0.00)	(0.00)	(0.00)	(0.00)	(0.00)
	cons. t	0.08	0.35	-0.49	0.25	-0.03	0.47
	p	(0.939)	(0.726)	(0.630)	(0.801)	(0.978)	(0.640)
	R^2	0.724	0.7692	0.8627	0.8155	0.8131	0.8552
$\sigma_{0.4i_1}$	coef. t	-0.31	0.47	1.24	-0.63	0.11	-0.36
	p	(0.759)	(0.645)	(0.227)	(0.535)	(0.917)	(0.719)
	cons. t	0.01	0.22	-0.05	0.04	0	0.14
	p	(0.995)	(0.827)	(0.960)	(0.968)	(0.999)	(0.89)
	R^2	0.0037	0.0083	0.0557	0.0149	0.0004	0.0051
$\sigma_{.4i_2}$	coef. t	0.92	1.11	0.43	-0.2	1.39	0.42
	p	(0.367)	(0.276)	(0.672)	(0.843)	(0.176)	(0.675)
	cons. t	-0.06	0.05	-0.23	0.13	-0.17	0.13
	p	(0.952)	(0.960)	(0.822)	(0.898)	(0.870)	(0.896)
	R^2	0.0314	0.0454	0.007	0.0015	0.0692	0.0069
$\sigma_{.8i} = -0.0833$	mean	-0.0042	-0.0016	-0.0059	-0.0037	-0.0043	-0.0055
	$\pm SE$	(0.0019)	(0.0008)	(0.0027)	(0.0016)	(0.0017)	(0.0021)

Software:Stata, version:SE 15.1

The six experiments' cycles from the 28 subspaces are employed to test the prediction of the three eigencycle sets ($\sigma_{.8i}$, $\sigma_{.4i_1}$, and $\sigma_{.4i_2}$) by OLE, respectively. The results from the six experiments are consistent:

- Among the 28 samples from the theoretical $\sigma_{.8i}$ (eigencycle set) and experimental L , there exists a significant linear dependence. The results show that $\sigma_{.8i}$ can independently be the principle component for the game dynamics.
- Importantly, we clearly observe the four cycles values, rated as (9:3:1:0) and predicted by $\sigma_{.8i}$ (see the red squares in Figure 3), indicating the discovery of the **fine structure** in the O'Neill game.
- Neither $\sigma_{.4i_1}$ nor $\sigma_{.4i_2}$ exists in significant linear dependence with experimental L . for the game dynamics. However, they are not invalid, as we later show that they lead to the **hyperfine structure**.

The supporting data of result 1:

The report of 'the discovery of the fine structure' is based on the consequence of the $\sigma_{.8i}$ by splitting the Ω^{15} cycle in 5 σ significant. This claim is supported by the data as following:

Figure 3 illustrates the ordinary least squares of the theoretical $\sigma_{.8i}$ and the six experimental L . Table 6 provides the results of the ordinary least squares between the six experiments and $\{\sigma_{.8i}, \sigma_{.4i_1}, \sigma_{.4i_2}\}$.

- On the claim of the discovery of the fine structure — The six subspaces of the six experiments, when observed together, yield 36 samples, and the result is strongly significant ($ttest$, $p=2.835 \times 10^{-15}$, $N=36$). More strictly, considering the concentration of the 8 dimension, omitting the 4- and 8-th dimension related subspaces, the result is strongly significant remained ($ttest$, $p=1.3802 \times 10^{-10}$, $N=24$). This stratifies the statistical significance of the five standard deviations (5σ , a threshold of $p \leq 2.87 \times 10^{-7}$) above background expectations, at 0. So, we claim the discovery of fine structure.
- Regarding the fine structure, the nine subspaces of the six experiments are observed together, giving us 54 samples. In this case, the result is strongly significant ($ttest$, $p=7.689 \times 10^{-7}$, $N=54$). We are not surprise by this relatively low significant, because the theoretical value is closer to background expectations, at 0.

Interpretation of result 1:

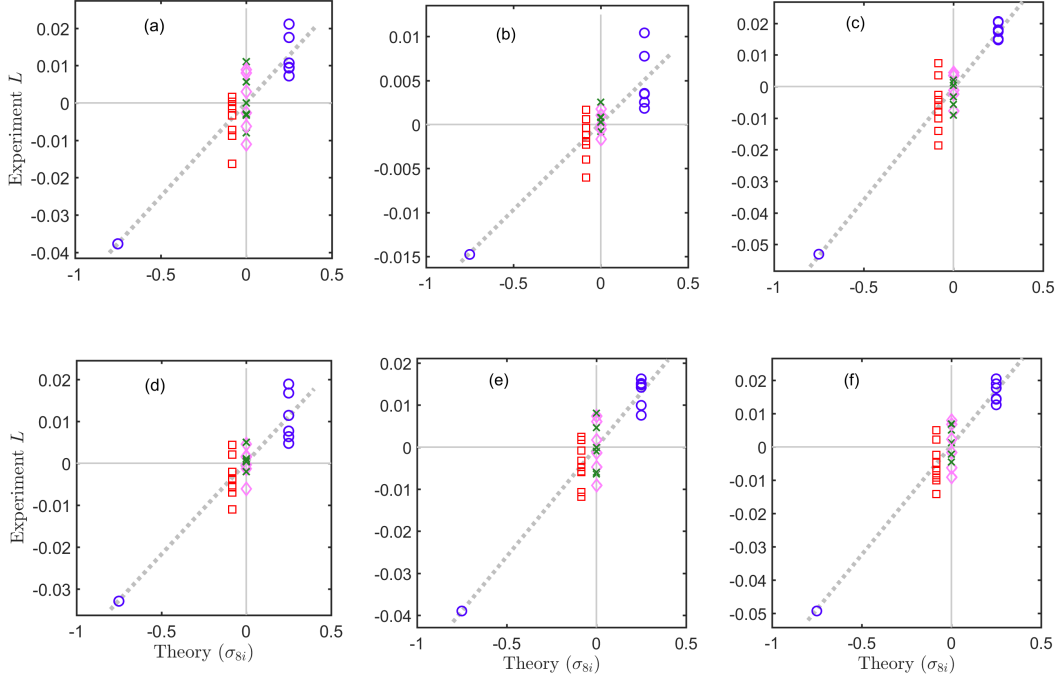


Figure 3: Linear regression to test the validity of the eigencycle set concept with $\sigma_{.8i}$ through the experiment. The 9:3:1:0 predicted by $\sigma_{.8i}$ is observed, which leads to the discovery of the fine structure of game dynamics. The experiment values for (a)–(f) are from the treatments ordered as in Table 3.

- **$\sigma_{.8i}$ as principal component** — The p value of the regression coefficient of $\sigma_{.8i}$ is close to 0.000, and the constant term cannot reject the 0 hypothesis. Thus, $\sigma_{.8i}$ is explanatory with respect to the main experimental results. We can regard $\sigma_{.8i}$ as the principal component in this system. $\sigma_{.8i}^{(15)}$ has the largest value, which is consistent with Binmore et al.'s suggestion [15] and confirmed by Wang and Xu [23] after converting the 4×4 game into a 2×2 payoff matrix. To our knowledge, the observed cycles in $\sigma_{.8i}^{(15)}$ are cutting-edge contributions on cycle measurement in the literature.
- **Discover the fine structure** — Beyond the $\Omega^{(15)}$ subspaces, $\sigma_{.8i}$ also predicts the cycle in the six subspaces, $\Omega^{(16,17,18,25,35,45)}$, and the nine two-dimensional subspaces, $\Omega^{(26,27,28,36,37,38,46,47,48)}$. These cycles are one-third or one-ninth in strength compared with $\Omega^{(15)}$'s cycle, which cannot be tested by earlier methods. However, the eigencycle set approach shows their significant existence. We call these the 'fine structure'.
- **Interpretation of $\sigma_{.4i}$ results** — The no-zero eigencycles in the $\sigma_{.4i_1}$ and $\sigma_{.4i_2}$ set are all independent of the first or fifth dimension. Hence, the experimental observed cycles in $\Omega^{(15,16,17,18,25,35,45)}$, which are obvious motions by $\sigma_{.8i}$, cannot be captured. As a result, neither $\sigma_{.4i_1}$ nor $\sigma_{.4i_2}$ can globally capture the entire 28-subspace motion reasonably.

4.2 Hyperfine structure

Result 2's description

We investigate $\sigma_{.4i_1}$ and $\sigma_{.4i_2}$ using the data. As per the main results, we find the hyperfine structure. In $\sigma_{.4i_1}$ and $\sigma_{.4i_2}$, the corresponding eigenvectors ($\xi_{.4i_1}$ and $\xi_{.4i_2}$) and components η_1 and η_5 are all 0. Hence, $\sigma_{.4i_1}$ and $\sigma_{.4i_2}$ have an effect only in the (2-3-4, 6-7-8) six-dimension subspace, which includes 15 two-dimensional subspaces where the eigencycles can exist. We use the two degenerate eigenvalues' eigencycle set ($\sigma_{.4i_1}, \sigma_{.4i_2}$) to build a pair of orthogonal bases as follows:

$$\begin{cases} \sigma_\alpha = (\sigma_{.4i_2} + \sigma_{.4i_1})/2, \\ \sigma_\beta = (\sigma_{.4i_2} - \sigma_{.4i_1})/2 \end{cases} \quad (10)$$

Table 7: Ordinary least squares results of experimental L_{P11} based on the eigencycle set

eigencycle set	coef. coef.	coef. t	coef. $p > t $	cons t	cons $p > t $	cons conf. interval
$\sigma_{.8i}$	0.057	27.36	0.000	0.11	0.910	[-0.001 0.001]
σ_α	0.006	4.43	0.003	-10.94	0.000	[-0.006 -0.004]
σ_β	0.005	3.31	0.030	-0.77	0.487	[-0.002 0.001]

Note: By the software Stata, version SE 15.1.

The mathematical explanations for the two bases are as follows:

- σ_α only relates to the (2-3-4, 6-7-8)-dimension outer-cross nine subspaces, $\Omega^{(26,27,28,36,37,38,46,47,48)}$. That is, σ_α has only nine components, but fully covers the nine two-dimensional subspace. Notably, as a strictly mathematical result, there exist only two values, and they are in opposition in σ_α .
- σ_β only relates to the (2-3-4, 6-7-8)-dimension inner-cross six subspaces, $\Omega^{(23,24,34,67,68,78)}$. That is, σ_β has only six components, but fully covers the six two-dimensional subspaces. Again, there exists only one value, and it is in σ_β .

The results of the experimental test are reported as follows:

- There exists significant linear dependence between the experimental L and σ_α . The constant term is also a consequence of $\sigma_{.8i}$. Hence, we have discovered the hyperfine structure.
- There exists significant linear dependence between the experimental L and σ_β . However, the constant term is zero and cannot be rejected.

Supporting data of result 2

The report of 'find evidence of hyperfine structure' is based on the statistical significant consequence of σ_α and σ_β on the fine structure due to $\sigma_{.8i}$. The supporting data are as following:

- Table 7 and Figure 4 show the supporting data. As the five treatments (labeled (O , IT , TI , II , and TT) in Table 3) have the same social state pattern (each two-dimensional subspace has four states), we thus pool the data under the label $P11$ -treatment.
- By regressing L_{P11} and $\sigma_{.8i}$ as well as σ_α and σ_β , we can obtain the result of the first, second, and third rows in Table 7, respectively, as shown in Figure 4.
 - L_{P11} and $\sigma_{.8i}$ have significant positive correlation (linear regression, $t=27.36$, $p=0.000$, $N=28$); See Figure 4(b).
 - L_{P11} and σ_α have significant positive correlation (linear regression, $t=4.43$, $p=0.003$, $N=9$), wherein the constant item is the influence of $0.8i$ on the nine points ($0.057 \times (-0.083) = -0.0047 \in \{-0.006, -0.004\}$); See Figure 4(b).
 - L_{P11} and σ_β have significant positive correlation (linear regression, $t=3.31$, $p=0.030$, $N=6$); See Figure 4(c).
- If sample by the experiments and the subspace simultaneously, we have larger sample size, and we get the same result.
 - If the σ_α 's nine subspaces of the six experiments are observed together, we obtain 54 samples. These samples can still be interpreted by σ_α with significance (Spearman's $\rho = 0.3554$, $p(2\text{-tailed}) = 0.00836$, $N=54$).
 - Similarly, with the σ_β 's six subspaces under the six experiments, we gain 36 samples, but the result is weakly significant (Spearman's $\rho = 0.31767$, $p(2\text{-tailed}) = 0.05903$, $N=36$).

Interpretation of result 2

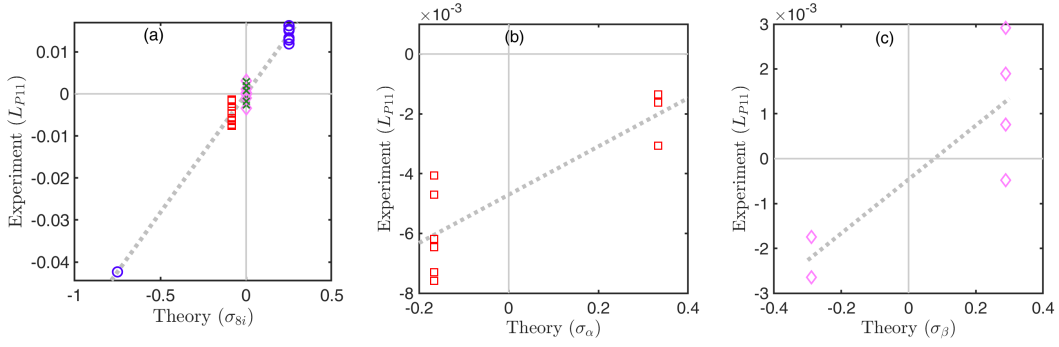


Figure 4: Fine structure and hyperfine structure of the cycles

Table 8: Multiple linear regression of experimental L_{P11} by $\sigma_{.8i}$, σ_{α} , and σ_{β}

L_{P11}	Coef.	Std. Err.	t	$P > t $	[95% Conf. Interval]	
$\sigma_{.8i}$.0565190	.0015589	36.25	.000	.0533014	.0597365
σ_{α}	.0057181	.0015589	3.67	.001	.0025006	.0089356
σ_{β}	.0045221	.0015778	2.87	.009	.0012656	.0077785
cons	-.0000876	.0002982	-0.29	.772	-.000703	.0005279

- **Finding the hyperfine structure** — L_{P11} and σ_{α} show significant correlation, indicating that σ_{α} can explain the hyperfine structure in the nine subspaces $\Omega^{(26,27,28,36,37,38,46,47,48)}$. Beyond $\sigma_{.8i}$, which predicts that the nine points have the same value, σ_{α} can also capture the differences among them. At the same time, the response mode reflected by σ_{α} is consistent with the best response mode in behavior game theory, which is also consistent with the win-stay-lose-shift mode in human decision-making [5].
- **Puzzle on σ_{β} 's result** — L_{P11} and σ_{β} have significant positive correlation, which cannot be explained by behavioral game theory. We suggest that this is the geometry factor effect, which is a natural result of the eight-dimensional presentation of the dynamics equation 5.

4.3 Eigencycle spectrum analysis

Descript of result 3:

With the eigencycle set as the orthogonal basis, we can explore high-dimensional dynamics through spectrum analysis in the form of Eq. (12). From the two subsections above, we can conclude that $\sigma_{.8i}$, σ_{α} , and σ_{β} simultaneously affect L_{P11} .

Supporting data of result 3:

Multiple regression analysis is a powerful technique used for predicting the unknown value of a variable from the known value of two or more variables- also called the predictors. Table 8 shows the supporting data. Multiple linear regression helps us interpret the experimental observation based on three theoretical eigencycle sets:

$$L_{P11} = 0.057\sigma_{.8i} + 0.006\sigma_{\alpha} + 0.005\sigma_{\beta} - 0.00009, \quad (11)$$

$$SE = \begin{matrix} (0.002) & (0.002) & (0.002) \end{matrix}$$

Function 11 is evidence that $\sigma_{.8i}$, σ_{α} , and σ_{β} have a significantly positive effect on L_{P11} . 0.057 is the partial regression coefficient of $\sigma_{.8i}$, which shows that, with the influence of σ_{α} and σ_{β} held constant, a one-unit increase in $\sigma_{.8i}$ increases L_{P11} by 0.057 units. Similar significance from α and β can be obtained.

Result 3's interpretation:

- Consistent with the two subsections above, the results in this subsection are also significant. That is, (1) The experimental observation is mainly determined by $\sigma_{.8i}$. (2) Compared with $\sigma_{.8i}$, σ_{α} and σ_{β} have a weaker but significant effect.
- Because of constant cannot reject 0 (linear regression, $t = -0.29$, $p = 0.772$), $\sigma_{.8i}$, σ_{α} and σ_{β} are ideal basic vector for spectral analysis.
- The eigencycle set can be an ideal basis for spectrum analysis, which is helpful for revealing the motion characteristics of high-dimensional game dynamics. The results in Table 6 are a significant illustration of this fact.

5 Discussion and conclusion

- Contributions. This study is unique in its discovery of the fine structure, the cycles in high dimension game, in the long-existed human behavior O'Neill game experiments. To our knowledge, it is the first report of the high dimensional cycle. We also find evidence on the existence of the hyperfine structure in the human cycling spectrum (see Figure 2). Meanwhile we have developed the eigencycle set decomposition approach. Through the invariant between the eigenvector components in a periodic dynamics system, by which we can test out the fine structure spectrum of human social cycling.
- On the implications of the discovery, we suggest that it may deeply influence our view on human game behavior. The conflict between the complex in experiment and the simply in theory seems visible. (1) The complex of the experiments game behaviors, which is high stochastic, discrete time, discrete strategy, non-linear, and high dimensional system, short time series, a extensive studied data which has existed more than 3 decades; (2) The simply of the theoretical predictors, which is differential, continue time, continue strategy space, and solvable by the tools from the standard concepts of the dynamics system theory. However, referring to the finding of the fine dynamics structure, they are compatible. It is well known that, the concepts and tools (e.g., stationary concept, Jacobian, eigensystem concept, Near periodic orbits, Poincare Section, Centre manifold theory) in the dynamics system theory are powerful. Now we see that, the reality and accuracy of the human behaviour game dynamics, then the evolutionary game theory, can be well improved along the standard dynamics system theory.
- On the implication of the eigencycle approach, we suggest that, it may be an improvement to the standard dynamics system theory. Not only can bring game dynamics system theory to experimental game dynamics systematically, it can be part of the standard analytical approach to where dynamics systems theory can be applied. This approach is bases on the invariant between two components of a given eigenvector, which, to our knowledge, is novel. Considering the widely application of the dynamics system theory, we hope to have more strictly mathematics study and potential empirical verification on the validation of the approach. Some details on the comparison of our approach with existed approach are shown in appendix section 6.7.2.
- We concern the questions raised during this study. Our finding have demonstrated the significant existence of cycles in high dimension game by the eigencycle approach. Although out of the scope of this study, there are some enigma remained,
 - The coefficients in Eq. (11) are not quantitatively explained in a clear manner. These coefficients may have physical meaning, such as the distribution of electrons in their orbit (eigenstates) obeying the Boltzmann distribution. But what governs the coefficients is unclear. On this question, some simulation results have shown that the coefficients is strongly depends on individual decision making methods [29], but the answer remains fuzzy.
 - The eigencycle approach offers new opportunities for formal dynamics model analysis, but also has its own limitations. First, it is based on linear approximation which is common in eigen system analysis. So, the application on large deviation condition needs caution. Second, we ignore the phase interfering between two components from two eigenvectors, but if in a delegation imaginary part of eigenvalue condition (although not common), the long-time and sufficient noise condition is necessary (see the proof in appendix section 6.2.2). So, for further strictly application, the boundary of the eigencycle approach needs further investigate.

- Our final concern is the central concept of game dynamics theory, or evolutionary game theory. Classical game theory has its central concept, Nash equilibrium, which reality, accuracy and applications have been well established. However, game dynamics theory has not such well established central concept. The ESS (evolution stable strategy) concept, which is mainly qualitative concept. Since recent experiments quantitative results accumulated [15, 6, 25, 9], a quantitative concept is more urgent. The fixed point theorem leads to the Nash equilibrium, which has become the central concept of the classical game statics theory. Have the finding the high dimensional game eigencycles, we calculate the 'invariant manifolds' and compare with eigencycles ant net transit. See appendix section 6.4 and 6.5 for details. As straightly impress, we suggest that 'invariant manifolds' could be a candidate as the central concept, which be used to capture complex dynamics and the long term behavior pattern of game dynamics. This concept, not only have solid mathematics background, but also can be verified in laboratory experiment. In the field of game dynamics theory and experiment, on dynamics pattern, there exists a common question [7].

In the background is a metaphysical question: what is a cycle?

By the fine structure out of the eigencycles in O'Neill games data, we wish the 'invariant manifolds' can be a concrete answer.

Acknowledgement: We thank O'Neill, Ken Binmore, and Yoshitaka Okano for providing the data. Thanks to Yijia Wang for her critical suggestion for Zhijian to obtain the pair of orthogonal basis (α, β) . The first author could be changed from Wang to Yao at any time during the revising and publishing processes of the top five economics journal. Wang designed the approach and Yao discovered the fine structure.

References

- [1] David Balduzzi, Marta Garnelo, Bachrach Xu, Wojciech Czarnecki, Julien Perolat, Max Jaderberg, and Thore Graepel. Evolutionary Rotation in Switching Incentive Zero-Sum Games. Proceedings of the 36 th International Conference on Machine Learning, Long Beach, California, PMLR 97, 2019.
- [2] Paolo Barucca, Mario Kieburg, and Alexander Ossipov. Eigenvalue and eigenvector statistics in time series analysis. EPL (Europhysics Letters), 129(6):60003, 2020.
- [3] James N Brown and Robert W Rosenthal. Testing the Minimax Hypothesis: A Re-examination of O'Neill's Game Experiment. Econometrica, 58(5):1065–1081, September 1990.
- [4] Noam Brown and Tuomas Sandholm. Superhuman ai for heads-up no-limit poker: Libratus beats top professionals. Science, 359(6374):418–424, 2018.
- [5] C.F. Camerer. Behavioral game theory: Experiments in strategic interaction. Princeton University Press, 2003.
- [6] Timothy N Cason, Friedman Daniel, and E. D. Hopkins. Cycles and instability in a rock–paper–scissors population game: A continuous time experiment. Review of Economic Studies, 1:1, 2014.
- [7] Timothy N. Cason, Daniel Friedman, and Ed Hopkins. An experimental investigation of price dispersion and cycles. Journal of Political Economy, 0(ja):null, 0.
- [8] Brian Dangerfield. System Dynamics. Springer, 2020.
- [9] D. Friedman and B. Sinervo. Evolutionary Games in Natural, Social, and Virtual Worlds. Oxford University Press, 2016.
- [10] Daniel Friedman. Evolutionary games in economics. Econometrica: Journal of the Econometric Society, pages 637–666, 1991.

- [11] Daniel Friedman. Evolutionary economics goes mainstream: a review of the theory of learning in games. Journal of Evolutionary Economics, 8(4):423–432, 1998.
- [12] Paulo Gonçalves. Behavior modes, pathways and overall trajectories: eigenvector and eigenvalue analysis of dynamic systems. System Dynamics Review: The Journal of the System Dynamics Society, 25(1):35–62, 2009.
- [13] Moshe Hoffman, Sigrid Suetens, Uri Gneezy, and Martin A Nowak. An experimental investigation of evolutionary dynamics in the rock-paper-scissors game. Scientific reports, 5(1):1–7, 2015.
- [14] John Van Huyck, Frederick Rankin, and Raymond Battalio. What does it take to eliminate the use of a strategy strictly dominated by a mixture? Experimental Economics, 2(2):129–150, 1999.
- [15] Joe Swierzbinski Ken Binmore and Chris Proulx. Does minimax work? an experimental study. The economic journal, 2001.
- [16] Zhiyue Lu and Oren Raz. Nonequilibrium thermodynamics of the markovian mpemba effect and its inverse. Proceedings of the National Academy of Sciences, 114(20):5083–5088, 2017.
- [17] Yoshitaka Okano. Minimax play by team. Games & Economic Behavior, 2013.
- [18] B. O’Neill. Nonmetric test of the minimax theory of two-person zerosum games. Proceedings of the National Academy of Sciences, 1987.
- [19] Marc R Roussel. Nonlinear Dynamics. Morgan & Claypool Publishers, 2019.
- [20] William H Sandholm. Population Games and Evolutionary Dynamics. MIT Press,, 2011.
- [21] Oriol Vinyals, Igor Babuschkin, Wojciech M Czarnecki, Michaël Mathieu, Andrew Dudzik, Junyoung Chung, David H Choi, Richard Powell, Timo Ewalds, Petko Georgiev, et al. Grandmaster level in starcraft ii using multi-agent reinforcement learning. Nature, 575(7782):350–354, 2019.
- [22] Yijia Wang, Xiaojie Chen, and Zhijian Wang. Testability of evolutionary game dynamics based on experimental economics data. Physica A: Statistical Mechanics and its Applications, 486:455 – 464, 2017.
- [23] Zhijian Wang and Bin Xu. Evolutionary Rotation in Switching Incentive Zero-Sum Games. arXiv e-prints, page arXiv:1203.2591, March 2012.
- [24] Zhijian Wang, Bin Xu, and Hai-Jun Zhou. Social cycling and conditional responses in the rock-paper-scissors game. Scientific reports, 4(1):1–7, 2014.
- [25] Bin Xu, Shuang Wang, and Zhijian Wang. Periodic frequencies of the cycles in *2imes2* games: evidence from experimental economics. European Physical Journal B, 87(2):46, 2014.
- [26] Bin Xu and Zhijian Wang. Dynamical pattern in a 2×2 game with human subjects (chinese). Available at SSRN 1729129, 2010.
- [27] Bin Xu and Zhijian Wang. Inertia of social rotation in laboratory 2×2 population games. Social ence Electronic Publishing, 2012.
- [28] Bin Xu and Zhijian Wang. Test maxent in social strategy transitions with experimental two-person constant sum 2×2 games. Results in Physics, 2:127 – 134, 2012.
- [29] Qinmei Yao. Theoretical analysis and experiment of dynamic structure of high dimensional game. Master’s thesis, 2021.
- [30] Shujie Zhou. Theory and experiment of dynamic structure in four strategy game. Master’s thesis, 2021.

6 Appendix

6.1 Appendix 1: Geometrical interpretation of eigencycle

Geometrical interpretation of eigencycle depend on the geometrical interpretation of complex eigenvectors in a system of differential equations.

A key element in dynamics system theory (modern control theory or linear systems theory) is the notion of the system eigenvalues, i.e., the eigenvalues of the Jacobian matrix. For simplicity, we restrict ourselves to the endogenous dynamics of the system. Suppose that an initial probability distribution can be expressed as a linear combination of the eigenvectors ξ as [16],

$$x(0) = c_1\xi_1 + c_2\xi_2 + \dots + c_n\xi_n, \quad (12)$$

wherein ξ_i is associated eigenvector of the eigenvalue λ_i ; The probability will evolve in time according to

$$x(t) = e^{\lambda_1 t}c_1\xi_1 + e^{\lambda_2 t}c_2\xi_2 + \dots + e^{\lambda_n t}c_n\xi_n, \quad (13)$$

Then the i component of x is

$$x_i(t) = \sum_{j=1}^n c_j \cdot \eta_{ij} \cdot \exp(\lambda_j t) \quad \{i, j\} \in \{1, 2, \dots, n\}. \quad (14)$$

For a given λ_j , the c_j is invariant for any components of the eigenvector ξ_j . Such that a given pair of the components will evolve respectively as

$$\begin{cases} x_m(t) &= c_j \cdot \|\eta_m\| \exp(\arg(\eta_m)) \cdot \exp(\lambda_j t) \\ x_n(t) &= c_j \cdot \|\eta_n\| \exp(\arg(\eta_n)) \cdot \exp(\lambda_j t) \end{cases} \quad (15)$$

Now we can show the geometric pattern of the evolution of x_m and x_n .

Suppose that the λ_i is pure imaginary number, in the two dimension (m,n) phase space, the curve is (1,1)-Lissajous, which is closed and periodic curve;

Meanwhile, the signed area is $\sigma^{(mn)}$ factor by c_j^2 as

$$c_j^2 \sigma^{(mn)} = \pi \cdot \|c_j\|^2 \cdot \|\eta_m\| \cdot \|\eta_n\| \cdot \sin(\arg(\eta_m) - \arg(\eta_n)), \quad (16)$$

Important is that for a given initial condition, the coefficients c_j is invariant along time. So, in all of the two dimensional subspace, the signed area is multiple by the constant $\|c_j\|^2$. That is

$$\frac{\sigma^{(mn)}}{\sigma^{(m'n')}} = \frac{\|\eta_m\| \cdot \|\eta_n\| \cdot \sin(\arg(\eta_m) - \arg(\eta_n))}{\|\eta'_m\| \cdot \|\eta'_n\| \cdot \sin(\arg(\eta'_m) - \arg(\eta'_n))} \quad (17)$$

$$= \frac{\Re(\eta_m)\Im(\eta_n) - \Re(\eta_n)\Im(\eta_m)}{\Re(\eta_{m'})\Im(\eta_{n'}) - \Re(\eta_{n'})\Im(\eta_{m'})} \quad (18)$$

Then the rate between the signed area is independent of c_j or λ_j in Eq. (14).

6.2 Appendix 2: Invariant between eigencycle and the angular momentum

The invariant between the eigencycle and the angular momentum is important in this study. Because, only having this invariant, we can using eigencycle as predictor for experimental angular momentum. Here, the eigencycle as predictor can be obtained by the eigenvector from dynamics equation, and the angular momentum can be obtained in time series.

In this section, we show that, the rate between the value of the eigencycle angular momentum L_{mn} and the value of the eigencycle σ_{mn} is **invariant** in respect to the subspace Ω^{mn} , in which $m, n \in \{1, 2, \dots, N\}$.

Main idea to prove the invariant is to calculate the angular momentum of the eigencycle explicitly.

6.2.1 Interfere of two components from the same eigenvector

First we need to describe the state $x(t)$ explicitly. Suppose that, in Eq. 13, the eigenvalue λ_i is not pure imaginary number, but a complex number $\lambda = \Re(\lambda) + i\Im(\lambda)$, wherein $\Re(\lambda) \neq 0, \Im(\lambda) \neq 0$. Then we have the m -th component

$$x_m(t) = c \cdot \exp(t \cdot (\Re(\lambda) + \Im(\lambda) \cdot i)) \cdot (\Re(\eta_m) + \Im(\eta_m) \cdot i)$$

herein we ignore the subscribe of c and λ . The real part of $x_m(t)$

$$\begin{aligned} x_m^r(t) &= c \cdot \Re(\eta_m) \cdot \exp(\Re(\lambda) \cdot t) \cdot \cos(\Im(\lambda) \cdot t) \\ &\quad - c \cdot \Im(\eta_m) \cdot \exp(\Re(\lambda) \cdot t) \cdot \sin(\Im(\lambda) \cdot t) \end{aligned} \quad (19)$$

Then the velocity of the state can be expresses as

$$\begin{aligned} \frac{d}{dt} x_m^r(t) &= c \cdot (\Re(\eta_m) \cdot \Re(\lambda) - \Im(\eta_m) \cdot \Im(\lambda)) \cdot \exp(\Re(\lambda) \cdot t) \cdot \cos(\Im(\lambda) \cdot t) \\ &\quad - c \cdot (\Im(\eta_m) \cdot \Re(\lambda) - \Re(\eta_m) \cdot \Im(\lambda)) \cdot \exp(\Re(\lambda) \cdot t) \cdot \sin(\Im(\lambda) \cdot t) \end{aligned} \quad (20)$$

Such, in (m,n) subspace, the instantaneous signed area change (the angular momentum) is

$$L_{mn}(t) = x_m^r(t) \times \frac{d}{dt} x_n^r(t) \quad (21)$$

$$= [x_m^r(t), x_n^r(t)] \times \left[\frac{d}{dt} x_m^r(t), \frac{d}{dt} x_n^r(t) \right]^T \quad (22)$$

$$= x_m^r(t) \cdot \frac{d}{dt} x_n^r(t) - x_n^r(t) \cdot \frac{d}{dt} x_m^r(t) \quad (23)$$

$$= c^2 \cdot \Im(\lambda) \cdot \exp(2 \cdot \Re(\lambda) \cdot t) \cdot (\Im(\eta_m) \cdot \Re(\eta_n) - \Re(\eta_m) \cdot \Im(\eta_n)) \quad (24)$$

So that, for any two sub-spaces $\Omega^{(mn)}$ and $\Omega^{(m'n')}$, we have the ratio of the the angular momentum at t as

$$R_{(mn,m'n')}(t) = \frac{L_{mn}(t)}{L_{m'n'}(t)} \quad (25)$$

$$= \frac{c^2 \Im(\lambda) \exp(2 \Re(\lambda) t) \cdot (\Im(\eta_m) \Re(\eta_n) - \Re(\eta_m) \Im(\eta_n))}{c^2 \Im(\lambda) \exp(2 \Re(\lambda) t) \cdot (\Im(\eta'_m) \Re(\eta'_n) - \Re(\eta'_m) \Im(\eta'_n))} \quad (26)$$

$$= \frac{\Re(\eta_m) \Im(\eta_n) - \Im(\eta_m) \Re(\eta_n)}{\Re(\eta'_m) \Im(\eta'_n) - \Im(\eta'_m) \Re(\eta'_n)} \quad (27)$$

$$= \frac{\sigma^{(mn)}}{\sigma^{(m'n')}} \quad (28)$$

So, we having following results.

Proposition 1

For a given eigenvector ξ , in all of the two dimension sub-spaces $\Omega^{(m,n)}$ at any given t , the rate between the instantaneous angular momentum value and eigencycle value is equal,

$$\frac{L_{mn}(t)}{\sigma^{(mn)}} = \mathbf{C}(t) \quad \forall (m, n) \in (1, 2, \dots, N) \quad (29)$$

Such that, we can expect that, for various subspace (m, n) , the average accumulated angular momentum L_{mn} divided by its $\sigma^{(mn)}$ is **invariant**,

$$\frac{1}{t_1 - t_0} \sum_{t=t_0}^{t_1} \frac{L_{mn}(t)}{\sigma^{(mn)}} = \frac{1}{t_1 - t_0} \sum_{t=t_0}^{t_1} \frac{L_{m'n'}(t)}{\sigma^{(m'n')}} = \mathbf{C} \quad \forall (m, n; m', n') \in (1, 2, \dots, N) \quad (30)$$

So, by take $\sigma^{(mn)}$ as predictor (independent variable) and take L_{mn} as the observation (dependent variables), the a linear regression line, with truncation term being 0, is expected.

6.2.2 Interfere of two components from two different eigenvector

For two given eigenvector ξ_1 and ξ_2 , in all of the two dimension sub-spaces the time average of the $L_{mn'} = 0$ in which $m \in \xi_1 \cap n' \in \xi_2$.

Denote the eigenvalue as λ , and $\Re(\lambda) := \delta$, $\Im(\lambda) := \omega$, the initial phase as ϕ , the instantaneous angular momentum at t can be expressed as,

$$L_{(m,n')}(t) = x \times \frac{dx}{dt} \quad (31)$$

$$= \Im \left(\left[c_1 \exp((\delta_1 + i\omega_1)t) A_m \exp(i\phi_m) \right]^\dagger \cdot \left[c_2 \exp((\delta_2 + i\omega_2)t) A_{n'} \exp(i\phi_{n'}) \right] \right) \quad (32)$$

$$= \Im \left(\left[c_1 \exp((\delta_1 - i\omega_1)t) A_m \exp(-i\phi_m) \right] \cdot \left[c_2 \exp((\delta_2 + i\omega_2)t) A_{n'} \exp(i\phi_{n'}) \right] \right) \quad (33)$$

$$= c_1 c_2 A_m A_{n'} \exp((\delta_1 + \delta_2)t) \Im \left(\exp(i((-\omega_1 + \omega_2)t - \phi_m + \phi_{n'})) \right) \quad (34)$$

$$= c_1 c_2 A_m A_{n'} \exp((\delta_1 + \delta_2)t) \sin \left((-\omega_1 + \omega_2)t - \phi_m + \phi_{n'} \right) \quad (35)$$

We set the term $c_1 c_2 \exp((\delta_1 + \delta_2)t) = 1$, which does not related to angular motion strictly. Then we have

1. Two inner components' interfere

When $m \in \xi_1$ and $n' \in \xi_1$ simultaneously, it is two inner components' interfere. As belong to same eigenvector and having same eigenvalue, then $\omega_1 = \omega_2$. Then the long time average of L is,

$$\overline{L_{(m,n')}} = \lim_{T \rightarrow \infty} \frac{1}{T} \int_0^T A_m A_{n'} \sin \left(-\phi_m + \phi_{n'} \right) dt \quad (36)$$

$$= \frac{1}{\pi} \sigma^{(m,n')} \quad (37)$$

is not 0. One can see that, the eigencycle value shown in main text can be re-archived, only less the constant $1/\pi$.

2. Two cross components' contribution in no delegation condition

When $\xi_1 \neq \xi_2$ and $\omega_1 \neq \omega_2$, the long time average,

$$\overline{L_{(m,n')}} = \lim_{T \rightarrow \infty} \frac{1}{T} \int_0^T A_m A_{n'} \sin \left((-\omega_1 + \omega_2)t - \phi_m + \phi_{n'} \right) \quad (38)$$

$$+ A_{m'} A_n \sin \left((-\omega_2 + \omega_1)t - \phi_{m'} + \phi_n \right) dt \quad (39)$$

$$= 0 \quad (40)$$

3. Two cross components' contribution in delegation condition without noise

When $\xi_1 \neq \xi_2$ and $\omega_1 = \omega_2$, this is the delegation condition. when facing $\lambda = 0.4i$ condition. In such condition, we can not strictly prove that the time average of the cross components contribution is zero.

$$\overline{L_{(m,n')}} = \lim_{T \rightarrow \infty} \frac{1}{T} \int_0^T A_m A_{n'} \sin \left((-\omega_\alpha + \omega_\beta) t - \phi_m + \phi_{n'} \right) \quad (41)$$

$$+ A_{m'} A_n \sin \left((-\omega_\beta + \omega_\alpha) t - \phi_{m'} + \phi_n \right) dt \quad (42)$$

$$= \lim_{T \rightarrow \infty} \frac{1}{T} \int_0^T A_m A_{n'} \sin \left(-\phi_m + \phi_{n'} \right) \quad (43)$$

$$+ A_{m'} A_n \sin \left(-\phi_{m'} + \phi_n \right) dt \quad (44)$$

$$\neq 0. \quad (45)$$

Because, in general case, the two equality, $A_{m'} A_n = A_m A_{n'}$ and $-\phi_m + \phi_{n'} = \phi_{m'} - \phi_n$, is not fulfilled.

4. Two components' cross contribution in delegation condition with noise

So called stochastic condition, we assume the white noise interrupts the system, and the system is rebuild, at this moment, the coefficient c_i and the initial phase ϕ_i changes randomly. As the eigen value and eigen vector remain unchanged, the system can be expressed as,

$$p(t) = \sum_i c_i \xi_i \exp(\lambda_i t + \theta_i).$$

$$\overline{L_{(m,n')}} = \lim_{K \rightarrow \infty} \frac{1}{\sum_{k=0}^K \tau_k} \sum_{k=0}^K \int_0^{\tau_k} A_m A_{n'} \sin \left(-(\phi_m + \theta_{1k}) + (\phi_{n'} + \theta_{2k}) \right) dt \quad (46)$$

$$= 0 \quad (47)$$

Herein, θ_{1k} the initial phase angle of ξ_1 after the k -th shock of noise. Following condition is necessary for this result hold:

- (a) White noise, and after a random interrupt, the θ_1 and θ_2 distribute between $[-\pi, \pi]$ equally.
- (b) Sufficient noise shock times limit, or saying there are sufficient times of the interrupt, that is $K \rightarrow \infty$.
- (c) Long time limit, there are sufficient long time of the time series, that is $\sum_k \tau_k \rightarrow \infty$.

In summery, the 0 comes out of the symmetry of the initial phase. In sufficient longtime, each $\theta_{1k} - \theta_{2k}$ has its oppose condition, then the average of the sinusoidal term is 0. In section 6.4 with a numerical verification approach, we provide an explanation on the results shown in Eq. (46).

Proposition 2

Interfere of two components from two different eigenvector is vanish, when following condition hold:

1. White noise condition: after a random interrupt, the initial phase of the two eigenvector distribute between $[-\pi, \pi]$ equally.
2. Sufficient noise shock: there are sufficient times of the interrupt, that is $k \rightarrow \infty$.
3. Long time limit: there are sufficient long time of the time series.

6.3 Appendix 4: The eigen system derivation and symmetry analysis

6.3.1 The eigen system derivation

For the given payoff matrix, assume x_i is the proposition of player 1 play strategy- i , the expected payoff for each strategy is,

$$\begin{pmatrix} U_{x_1} \\ U_{x_2} \\ U_{x_3} \\ U_{x_4} \\ U_{y_1} \\ U_{y_2} \\ U_{y_3} \\ U_{y_4} \end{pmatrix} = \begin{pmatrix} y_1 - y_2 - y_3 - y_4 \\ y_3 - y_2 - y_1 + y_4 \\ y_2 - y_1 - y_3 + y_4 \\ y_2 - y_1 + y_3 - y_4 \\ x_2 - x_1 + x_3 + x_4 \\ x_1 + x_2 - x_3 - x_4 \\ x_1 - x_2 + x_3 - x_4 \\ x_1 - x_2 - x_3 + x_4 \end{pmatrix}$$

Herein, U_{x_i} is the payoff of the strategy x_i . Then, the mean payoff $\overline{U_X}$ and $\overline{U_Y}$ for the two populations (players) can be expressed respectively as

$$\begin{aligned} \overline{U_X} &= -x_1 (y_2 - y_1 + y_3 + y_4) - x_2 (y_1 + y_2 - y_3 - y_4) \\ &\quad - x_3 (y_1 - y_2 + y_3 - y_4) - x_4 (y_1 - y_2 - y_3 + y_4) \end{aligned} \quad (48)$$

$$\begin{aligned} \overline{U_Y} &= y_1 (x_2 - x_1 + x_3 + x_4) + y_2 (x_1 + x_2 - x_3 - x_4) \\ &\quad + y_3 (x_1 - x_2 + x_3 - x_4) + y_4 (x_1 - x_2 - x_3 + x_4) \end{aligned} \quad (49)$$

Referring to the replicator dynamics, shown in main text as Eq. (5), the expanded form is:

$$\begin{aligned} \frac{d}{dt}x_1 &= x_1 (y_1 - y_2 - y_3 - y_4 + x_1 (y_2 - y_1 + y_3 + y_4) + x_2 (y_1 + y_2 - y_3 - y_4) \\ &\quad + x_3 (y_1 - y_2 + y_3 - y_4) + x_4 (y_1 - y_2 - y_3 + y_4)) \end{aligned} \quad (50)$$

$$\begin{aligned} \frac{d}{dt}x_2 &= x_2 (y_3 - y_2 - y_1 + y_4 + x_1 (y_2 - y_1 + y_3 + y_4) + x_2 (y_1 + y_2 - y_3 - y_4) \\ &\quad + x_3 (y_1 - y_2 + y_3 - y_4) + x_4 (y_1 - y_2 - y_3 + y_4)) \end{aligned} \quad (51)$$

$$\begin{aligned} \frac{d}{dt}x_3 &= x_3 (y_2 - y_1 - y_3 + y_4 + x_1 (y_2 - y_1 + y_3 + y_4) + x_2 (y_1 + y_2 - y_3 - y_4) \\ &\quad + x_3 (y_1 - y_2 + y_3 - y_4) + x_4 (y_1 - y_2 - y_3 + y_4)) \end{aligned} \quad (52)$$

$$\begin{aligned} \frac{d}{dt}x_4 &= x_4 (y_2 - y_1 + y_3 - y_4 + x_1 (y_2 - y_1 + y_3 + y_4) + x_2 (y_1 + y_2 - y_3 - y_4) \\ &\quad + x_3 (y_1 - y_2 + y_3 - y_4) + x_4 (y_1 - y_2 - y_3 + y_4)) \end{aligned} \quad (53)$$

$$\begin{aligned} \frac{d}{dt}y_1 &= -y_1 (x_1 - x_2 - x_3 - x_4 + y_1 (x_2 - x_1 + x_3 + x_4) + y_2 (x_1 + x_2 - x_3 - x_4) \\ &\quad + y_3 (x_1 - x_2 + x_3 - x_4) + y_4 (x_1 - x_2 - x_3 + x_4)) \end{aligned} \quad (54)$$

$$\begin{aligned} \frac{d}{dt}y_2 &= -y_2 (x_3 - x_2 - x_1 + x_4 + y_1 (x_2 - x_1 + x_3 + x_4) + y_2 (x_1 + x_2 - x_3 - x_4) \\ &\quad + (y_3 (x_1 - x_2 + x_3 - x_4) + y_4 (x_1 - x_2 - x_3 + x_4))) \end{aligned} \quad (55)$$

$$\begin{aligned} \frac{d}{dt}y_3 &= -y_3 (x_2 - x_1 - x_3 + x_4 + y_1 (x_2 - x_1 + x_3 + x_4) + y_2 (x_1 + x_2 - x_3 - x_4) \\ &\quad + y_3 (x_1 - x_2 + x_3 - x_4) + y_4 (x_1 - x_2 - x_3 + x_4)) \end{aligned} \quad (56)$$

$$\begin{aligned} \frac{d}{dt}y_4 &= -y_4 (x_2 - x_1 + x_3 - x_4 + y_1 (x_2 - x_1 + x_3 + x_4) + y_2 (x_1 + x_2 - x_3 - x_4) \\ &\quad + y_3 (x_1 - x_2 + x_3 - x_4) + y_4 (x_1 - x_2 - x_3 + x_4)) \end{aligned} \quad (57)$$

The rest point of the game can be solved with the concentration

$$0 < x_i, y_i < 1, \quad i \in [1, 2, 3, 4]$$

Then the mixed strategy solution x^* can be archive,

$$x^* := (x_1^*, x_2^*, x_3^*, x_4^*, y_1^*, y_2^*, y_3^*, y_4^*) = (2/5, 1/5, 1/5, 1/5, 2/5, 1/5, 1/5, 1/5).$$

The Taylor series expansion of dx/dt about this point x^* is:

$$\frac{d}{dt}x_i = \left. \frac{d}{dt}x_i \right|_{x^*} + \frac{\partial(\frac{d}{dt}x_i)}{\partial x_j}(x_j - x_j^*) + O(\Delta x^2)$$

We assume v sufficiently smooth and differentiable for the Taylor expansion to exist. At a critical point, the first term of the Taylor expansion vanishes (by definition). We consider only the second term. At this points, the Jacobian matrix (character matrix)

$$\mathbf{J} \Big|_{x^*} = \begin{bmatrix} \frac{\partial(\frac{d}{dt}x_1)}{\partial x_1} & \dots & \frac{\partial(\frac{d}{dt}x_1)}{\partial x_8} \\ \vdots & \ddots & \vdots \\ \frac{\partial(\frac{d}{dt}x_8)}{\partial x_1} & \dots & \frac{\partial(\frac{d}{dt}x_8)}{\partial x_8} \end{bmatrix} \Big|_{x^*} \quad (58)$$

$$= \frac{1}{25} \begin{bmatrix} 2 & 2 & 2 & 2 & 12 & -8 & -8 & -8 \\ 1 & 1 & 1 & 1 & -4 & -4 & 6 & 6 \\ 1 & 1 & 1 & 1 & -4 & 6 & -4 & 6 \\ 1 & 1 & 1 & 1 & -4 & 6 & 6 & -4 \\ -12 & 8 & 8 & 8 & -2 & -2 & -2 & -2 \\ 4 & 4 & -6 & -6 & -1 & -1 & -1 & -1 \\ 4 & -6 & 4 & -6 & -1 & -1 & -1 & -1 \\ 4 & -6 & -6 & 4 & -1 & -1 & -1 & -1 \end{bmatrix} \quad (59)$$

Using the Characteristic polynomial, this character matrix is diagonalizable. From which, the eigenvalue and eigenvector set can be archived explicitly. <https://matrixcalc.org/en/vectors.html>

6.3.2 Eigen system and invariant manifold

The suggestion on the invariant manifold can be a candidate of the central concept is based on the bridge between the Eigen system and invariant manifold, both of which are concepts in dynamical systems theory. [19]

Eigen system indicates the eigenvalues and eigenvectors, and their related concepts, like eigenspace and eigendirection. An invariant manifold is a topological manifold that is invariant under the action of the dynamical system.

Around the rest point, the eigenvalues and eigenvectors of the matrix determine the local behavior dx/dt . Positive eigenvalues indicate that dx/dt is directed away from the critical point (a repelling eigendirection) and negative values the opposite (an attracting eigendirection). A complex conjugant pair of eigenvalues indicate that dx/dt spirals in or out, depending on the sign of the real part of the eigenvalues. Thus the linear approximation of dx/dt near the rest point is characterized by the eigenvalues and eigenvectors.

Application of the eigenvalues and eigenvectors is dramatically important.

- The eigenvalues may be used to classify the type of the rest point. In the textbook for game dynamics [20], Bill Sandholm has emphasised the stable manifold theorem, which rely on the real part of the eigenvalues. The stable manifold theorem says that within some neighborhood of x^* , there is k dimensional local stable manifold on which solutions converge to x^* at an exponential rate, and an $n - k$ dimensional local unstable manifold on which solutions converge to x^* at an exponential rate if time is run backward.
- The eigenvectors may be used to find its invariant manifolds. Based on the linearized stability analysis, the eigenspaces (subspaces of the full phase space spanned by eigenvectors) can be classified as
 - The stable eigenspace, which is the space spanned by the eigenvectors whose corresponding eigenvalues have negative real parts.
 - The unstable eigenspace, which is the space spanned by the eigenvectors whose corresponding eigenvalues have positive real parts.

- The centre eigenspace, is the space spanned by the eigenvectors whose corresponding eigenvalues have a real part of zero.

Along such classification [19], the O'Neill game, except the real part, the eigenvectors forms the 6 dimension **centre eigenspace**.

In this view, the 28 subspaces are the projection of the invariant manifold in the centre eigenspace, which are of the **central manifold**.

6.3.3 The Lissajous figure and its statistics meaning

Lissajous figure is the pattern produced by the intersection of two sinusoidal curves, the axes of which are at right angles to each other. In our study case, any two components from an eigenvector will perform as 1:1 Lissajous figure. In general condition, the Lissajous figures are of elliptical shape in the subspace. The appearance of the figure is highly sensitive to the amplitudes and the phase difference.

The shape of the curve serving to identify the characteristics of the signals. The shape is helpful to identify the relationship of the two signals. Its statistics meaning in dynamics processes, as typical examples, are dependent on the phase difference between the two sinusoidal signals:

- $\phi_m - \phi_n = 0$, the Lissajous figure is a straight line with an inclination with positive x-axis, the two variable is positive depend.
- $\phi_m - \phi_n = \pi$, the Lissajous figure is a straight line with an inclination with negative x-axis, the two variable is negative depend.
- $\phi_m - \phi_n = \pi/2$, Counter clockwise cycle, m is causal of n , statistically, when m appears then n appears.
- $\phi_m - \phi_n = -\pi/2$, the Lissajous figure is in circular shape, clockwise cycle, n is causal of m , statistically, when n appears then m appears.

6.3.4 The eigen system symmetry

The symmetry of the game bases on the Jacobian (character matrix) of the game. The result is significant after investigating the eigenvectors.

Real eigenvalues and their eigenvectors Notice that, the sum of the columns is

$$(1/5, 1/5, 1/5, 1/5, -1/5, -1/5, -1/5, -1/5)$$

which indicates the game value for player 1 is $1/5$ and player 2 is $-1/5$. These two values are the eigen value of the Jacobian; Meanwhile, their related eigenvectors indicates the Nash distribution [20].

Image eigenvalues and their complex eigenvectors There are three pairs of image eigenvalue. Their related eigenvectors involves in the cross interactions between the two populations.

- in 1-st and 5-th dimension, only $.8i$ eigenvector involves. The two $.4i$ eigenvector have no consequence on the subspace $\Omega^{(mn)}$ when m or n includes 1 or 5; Because, the $.4i$ related eigenvector components of are 0 in 1 and 5.
- The cycles of the crossover of the 2-3-4 and 6-7-8 dimensions.
- The cycles of the inner 2-3-4 or of the inner 6-7-8 dimensions.

6.4 Appendix 6: Verification of the invariant manifold and eigencycle

Along the concept of the invariant manifold, we can use the dynamics system equations set, shown in Eq. (50), to calculate the solution for approximate invariant manifold. The algorithm in Matlab language is shown following.

As the results, the invariant manifold are approximately shown in figure 6. Obviously, the patterns support our abstract of the eigen cycle. Several visible results are:

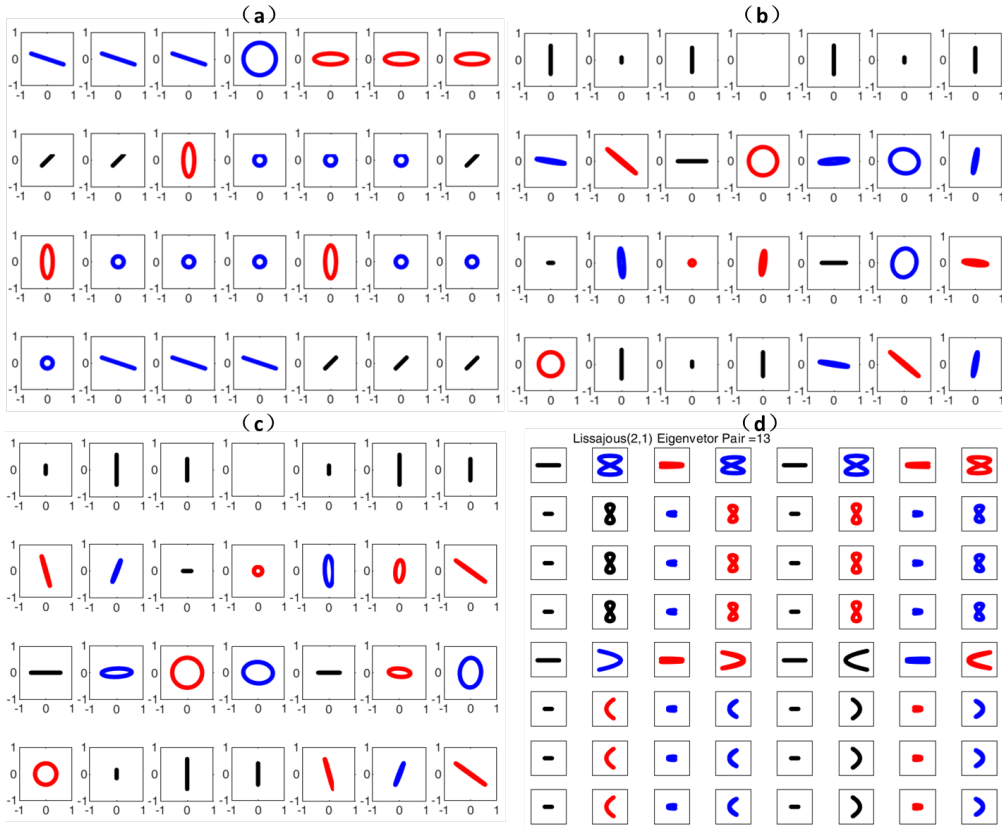


Figure 5: Eigencycles in the 28 subspaces from the 3 image eigenvectors (a) $0.8i$ (b) $0.4i_1$ (c) $0.4i_2$ (d) an illustration of 2:1-lissajous figure.

1. The cycle or ellipse shape exactly similar to the Lissajous orbit;
2. The cycle or ellipse area size exactly similar to the Lissajous orbit;
3. The ellipse major axis has some inclination angle with positive x-axis.
4. The consequence of multi-frequency, the eigenvalue as $4i$ and $8i$, appears as (1:2)-Lissajous orbit.

Notice that, this dynamics system do not satisfy the requirement of the central manifold requirement, because, one of the eigenvalue is positive. The (1:2)-Lissajous orbit pattern shown in figure 6 is initial condition depended. On average, the zero hypnosis in Eq 46 about Two components cross contribution in delegation condition with noise.

```
% Approximate invariant manifold for replicator dynamics equation.
% Matlab 2019b
function [T,Y] = tmp202106122()

tspan = [0 30];
ini = [2 1 1 1 2 1 1 1]/5 + 0.001*rand(1,8);
initial_pos = [ini(1:4)/sum(ini(1:4)) ini(5:8)/sum(ini(5:8))];

[T,Y] = ode45(@osc,tspan,initial_pos);
figure;plotmatrix(Y,','.-'); title(num2str(a))

function dydt = osc(t,y)
dydt = ...
[ y(1)*(5*y(5) - 5*y(6) - 5*y(7) - 5*y(8) + y(1)*(5*y(6) - 5*y(5) + 5*y(7) + 5*y(8)) + ...
y(2)*(5*y(5) + 5*y(6) - 5*y(7) - 5*y(8)) + y(3)*(5*y(5) - 5*y(6) + 5*y(7) - 5*y(8)) + ...
y(4)*(5*y(5) - 5*y(6) - 5*y(7) + 5*y(8)))
y(2)*(5*y(7) - 5*y(6) - 5*y(5) + 5*y(8) + y(1)*(5*y(6) - 5*y(5) + 5*y(7) + 5*y(8)) + ...
y(2)*(5*y(5) + 5*y(6) - 5*y(7) - 5*y(8)) + y(3)*(5*y(5) - 5*y(6) + 5*y(7) - 5*y(8)) + ...
y(4)*(5*y(5) - 5*y(6) - 5*y(7) + 5*y(8)))
```

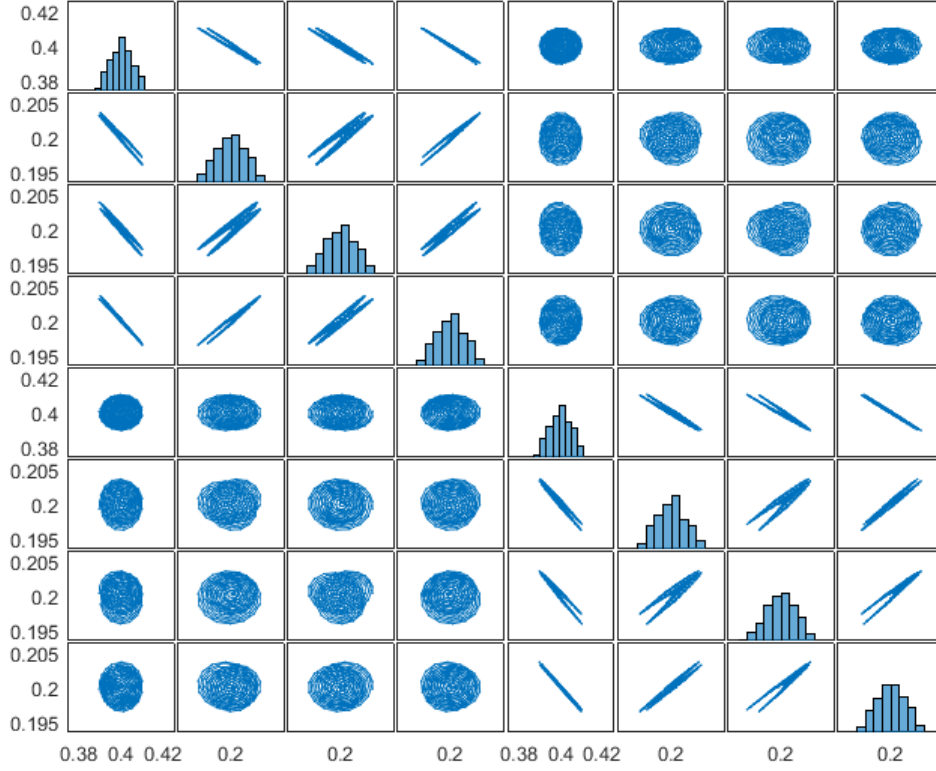


Figure 6: Projection of the 8 dimension approximate invariant manifold trajectory on the 28 sub-spaces. This is the matrix plot, each subplot presents an two variable (m, n) interfere. The horizon-axis indicates m -dimension from left to right is 1 to 8, and vertical-axis indicates n -dimension from up to down is 1 to 8.

```

y(3)*(5*y(6) - 5*y(5) - 5*y(7) + 5*y(8) + y(1)*(5*y(6) - 5*y(5) + 5*y(7) + 5*y(8)) + ...
y(2)*(5*y(5) + 5*y(6) - 5*y(7) - 5*y(8) + y(3)*(5*y(5) - 5*y(6) + 5*y(7) - 5*y(8)) + ...
y(4)*(5*y(5) - 5*y(6) - 5*y(7) + 5*y(8)))
y(4)*(5*y(6) - 5*y(5) + 5*y(7) - 5*y(8) + y(1)*(5*y(6) - 5*y(5) + 5*y(7) + 5*y(8)) + ...
y(2)*(5*y(5) + 5*y(6) - 5*y(7) - 5*y(8) + y(3)*(5*y(5) - 5*y(6) + 5*y(7) - 5*y(8)) + ...
y(4)*(5*y(5) - 5*y(6) - 5*y(7) + 5*y(8)))
-y(5)*(5*y(1) - 5*y(2) - 5*y(3) - 5*y(4) + y(5)*(5*y(2) - 5*y(1) + 5*y(3) + 5*y(4)) + ...
y(6)*(5*y(1) + 5*y(2) - 5*y(3) - 5*y(4)) + y(7)*(5*y(1) - 5*y(2) + 5*y(3) - 5*y(4)) + ...
y(8)*(5*y(1) - 5*y(2) - 5*y(3) + 5*y(4)))
-y(6)*(5*y(3) - 5*y(2) - 5*y(1) + 5*y(4) + y(5)*(5*y(2) - 5*y(1) + 5*y(3) + 5*y(4)) + ...
y(6)*(5*y(1) + 5*y(2) - 5*y(3) - 5*y(4)) + y(7)*(5*y(1) - 5*y(2) + 5*y(3) - 5*y(4)) + ...
y(8)*(5*y(1) - 5*y(2) - 5*y(3) + 5*y(4)))
-y(7)*(5*y(2) - 5*y(1) - 5*y(3) + 5*y(4) + y(5)*(5*y(2) - 5*y(1) + 5*y(3) + 5*y(4)) + ...
y(6)*(5*y(1) + 5*y(2) - 5*y(3) - 5*y(4)) + y(7)*(5*y(1) - 5*y(2) + 5*y(3) - 5*y(4)) + ...
y(8)*(5*y(1) - 5*y(2) - 5*y(3) + 5*y(4)))
-y(8)*(5*y(2) - 5*y(1) + 5*y(3) - 5*y(4) + y(5)*(5*y(2) - 5*y(1) + 5*y(3) + 5*y(4)) + ...
y(6)*(5*y(1) + 5*y(2) - 5*y(3) - 5*y(4)) + y(7)*(5*y(1) - 5*y(2) + 5*y(3) - 5*y(4)) + ...
y(8)*(5*y(1) - 5*y(2) - 5*y(3) + 5*y(4)))
];
end
end

```

end

6.5 Appendix 7: Verification of the net transit and eigencycle

- **Definition**

Net transit (denoted as T) relates to the strategy probability transition, which is a concept in stochastic processes. The strategy probability transition from state m to n , which can be denoted

as a Markovian matrix element $A_{m,n}$. Denotes the stationary distribution as vector ρ , the Net transit can be presented by the net transit matrix and defined as [26]

$$T_{m,n} = \rho_m A_{m,n} - \rho_n A_{m,n}^T = \rho_m A_{m,n} - \rho_n A_{n,m},$$

which describes the net probability current T from state- m to state- n .

Assume a system has N independent states total, this definition has following property.

- If the system is in detail balance condition,

$$T_{m,n} = 0, \quad \forall m, n \in N;$$

- If observed $T_{m,n} > 0$, there exists net current from m to n ;
- If observed $T_{m,n} < 0$, there exists net current from n to m ;
- The net transit matrix is anti-symmetry, $T_{m,n} = -T_{n,m}$.

Using the data shown in main text Table 3, we can conduct following two calculation and present in matrix plotting,

- The net transit matrix T_{mn} ,
- The experimental angular momentum L_{mn} .

- **Result**

The results are shown in figure 7. In this plot, we use all of the times series, total about 13 thousands transition. The net transit appears in $T_{5,1}$ and $L_{5,1}$, which means the probability of the net transit counted is 500 in about 13 thousands transit.

Importantly, the comparison shows us the physical meaning of the angular momentum, and then the eigencycle, both of the value and the signal.

6.6 Appendix 5: Data and dynamics model valid

- Data valid

The two-person fixed-paired discrete time game experiment for testing the dynamical pattern. The literature [28] shows that testing the dynamical pattern in a long-run fixed-paired 2×2 game in a strategy space is possible. Given the myopic nature of human behavior, we expect a cyclical pattern. Although the time series is highly stochastic, we can test dynamics behavior using the time reserve asymmetry measurement, much like the velocity field or angular momentum measurement [22]. In a one population symmetry *4times4* game experiments [30], and in a one population symmetry 5×5 game experiments [29], we have obtained that, eigencycle approach valid.

- Dynamics valid

Employing replicator dynamics and perturbation expansion to the model. Replicator dynamics is the earliest developed model. Evidence shows that the model, as well as the perturbation expansion, can capture the main character of dynamics behavior [25]. Hence, both replicator dynamics and perturbation expansion can be part of standard analysis in mathematics, thereby offering a clear and practical picture of the eigen system.

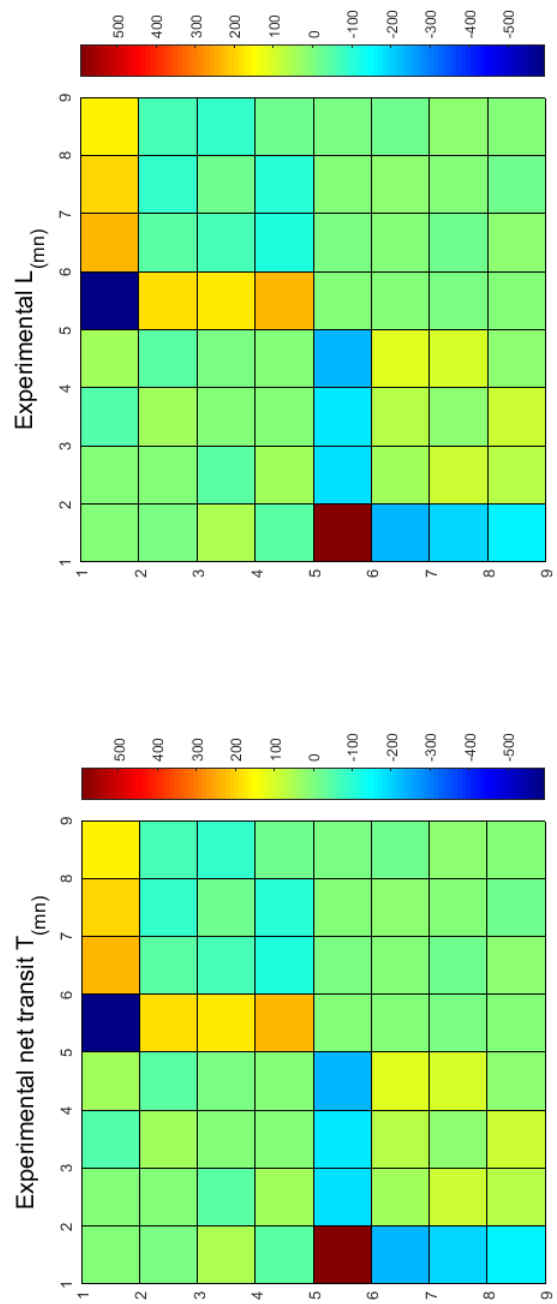


Figure 7: Verification of the net transit and eigencycle matrix. The horizon-axis indicates m -dimension from left to right is 1 to 8, and vertical-axis indicates n -dimension from up to down is 1 to 8.

6.7 Appendix 3: Related works

6.7.1 Related works on the evolutionary game theory and experiment

[**Question**] Main result of this paper is finding the dynamics cycle in high dimension strategy interaction system (game). Interestingly, in quite recently paper [7], the authors clearly pointed out that detecting cycles in high dimensions game remains an open question. This is the first question.

The second question is a basic in the field of evolutionary game theory and experiment. The question is excellently abstracted by Dan Friedman and his colleague as [7]

In the background is a metaphysical question: what is a cycle?

[**History**] In fact, the questions have last for nearly three decades since early 1990s when evolutionary game theory came into economics [10, 11]. The time line on the questions can be divided into periods.

- **No cycle observed period** is during 1990s-2000s, the common knowledge was, like mentioned in the textbook namely behavior game experiments [5], evolutionary approach fit biology, or culture evolution, not fit to describe quickly human game strategy interaction behavior. Such description is based on the previous experiments reports.
- **Confirm cycle existence period** since 2010s, which mainly base on rock-paper-scissors game or 2×2 game experiment, no high dimension cycles reports.
 - [13] reported observation of distribution differs from Nash equilibrium concept but fit evolutionary dynamics in RPS game experiment.
 - [6] reported observation of cycles in the continuous time setting RPS game experiment;
 - [25] reported observation of cycles in classical discrete time setting RPS game experiment;
 - [25] reported observation of cycles in classical discrete time randomly matching 2×2 game experiment;
- **Quantifying cycle measurement**, whenever report cycle existence, is necessary. Following measurements have been shown
 - CRI (cycle rotation index) in RPS [6]
 - period of cycle (or frequency of cycle) in 2×2 [25].
 - velocity field of cycle in RPS [22]
 - angular momentum of cycle in RPS [22]
 - net transit between states in 2×2 game [26].
- **Unifying cycle measurement** has been concerned naturally. The unify between velocity and angular momentum [22], between CRI and frequency of cycle [25], has shown us the inner consistency of these measurements.

[**Summery**]

- On the open question about how to identify high dimension game, we hope, our finding of the eigencycle is an appreciate answer.
- On the metaphysical question about what is a cycle, we suggest, with more accuracy results of more 'unexpected' observations from deeper theoretical analysis and more experiments conduction, as the full picture being clear, the answer will become clearer and clear.

6.7.2 Related works on the dynamics system theory

Our study is not lonely on using the concepts and tools from the dynamics system theory to study human game dynamics behavior in laboratory experiments since 1990s. The framework and the method is common, which has been the standard narration mode [9, 20].

The framework to describe the dynamics includes two concepts,

1. Game dynamics study has its own conventions since its very beginning, by describing the dynamical systems with ODE (ordinary differential equations) mathematically;
2. The phase space of a dynamical system is the collection of all possible world-states of the system in question. Each world state represents a complete snapshot of the system at some moment in time;

The technology methods, as well as its illustrations in existed literature, are:

1. solve the equations for the rest points (or singularity point, equilibrium, stationary state);
2. analysis the evolutionary trajectory in the phase space;
3. solve the character matrix (Jacobian) for eigen system including eigenvalues and eigenvectors;
4. by real part of the eigenvalue, analysis the stability ;
5. by imagine part of the eigenvalue, evaluate the periods of limit cycle near the rest point;
6. linear decomposition the system by the eigen system, namely spectrum analysis.

To our knowledge, none of the literature, at least in game dynamics theory and experiment fields, has focus on the eigenvector structure.

Eigen system as analysis framework and toolbox Basing on linear approximation decomposition approach, eigenvalue and eigenvector are the corner stones for the formal dynamics system analysis framework. The eigencycle approach, which is based on the eigenvector components, belongs to this framework. Following, we revisit related approach in the framework.

- Eigenvalue used as an analysis tool is common for spectrum analysis and stability analysis. As well known that, its real part determines the stability, meanwhile, its imaginary part determine the frequency of the vibration mode.
- Using real eigenvector is common too, for example, eigenvectors indicates distribution [9, 20]. The dynamic decomposition weights (DDW) approach [8] using only the real part (not the imagine part) of the components of an eigenvector.
- Using the complex characters of an eigenvector component is rare. Two welcome exceptions are (1) It has noticed the coupling of the eigenvalues to eigenvectors will lead to phase shift [12], but ignore the phase interfere between two eigenvector components. (2) Scholars have suggest to borrow quantum physics concepts on eigenvector to investigate [2], but do not provide practical way or example.

Comparing with existed approach, our eigencycle approach is using the phase interfere between the eigenvector components. The potential power of the eigencycle approach is encouraged by our surprisingly finding the high dimensional fine dynamics structure our of decades long fundamental human subject game experiments.

Advantage of the eigencycle

- Eigencycle can be more efficient bridge between theory and experiment. In this study, we have illustrated the consistence of the eigencycle with following two existed measurement,
 1. the angular momentum measurement L , details are shown in section 6.4.
 2. the net transit measurement T , details are shown in section 6.5

But different from these two measurements, the eigencycle set can be deviate from the eigenvectors, which can be explicitly calculate out of the dynamics equation set.

- Eigencycle can be an efficient tube to bring in the concepts and tools, for game dynamics research. The concepts and tools has already in the dynamics system theory, like central manifold theorem, invariant set theorem, eigen space, the invariant manifold and among others, we believe, will significantly improve our design and analysis experiment and theory .

6.7.3 Related works on the dynamics cycle in O'Neill game

The eigencycle approach bases on the eigenvector, which rooting in dynamical system theory. We review the literature history in O'Neill game analysis to explain the advance made by the eigencycle approach. As illustrated in figure 8, an extending explanation are follow.

- Subfigure (1987) — The above game matrix designed by O'Neill is historic. It provides the first evidence on the reality and accuracy of the mixed strategy Nash equilibrium. Subfigure (1978) — The evolutionary character, when transited to a 2×2 game, can be captured by the replicator dynamics equation, as first noted in 1978 [20].
- Subfigure (2001) — This figure is derived from [15]. Regarding geometric cyclic behavior, where it was first presented, the authors conducted an experiment of 150 rounds, repeated per session, with a total of 13 sessions. However, their measurement does not yield results with significant confidence from the 13 sessions. Instead, they report manually selected 150 rounds with likely-cycle trajectory only.
- Subfigure (2012) — Based on the method to concentrate the 4×4 zero sum game to a 2×2 zero sum game, Wang and Xu report the existence of a cycle in the O'Neill game by testing the accumulated angular momentum [23]. As shown in Subfigure (2012), for all the 13 sessions, the accumulated angular momentum is constantly declining. That is, clockwise rotation is robust for all 13 sessions. However, as the second, third, and fourth strategies are concentrated in one strategy, the authors miss the high-dimensional cyclical characters. To elaborate, as all the second, third, and fourth strategies of player A and player B are combined into one strategy, namely, the down-strategy for A and down-strategy for B, the cyclic behavior in the combined strategies is missed.
- Subfigure (2020) — By applying the eigencycle set analysis for the O'Neill game, there is no need to resort to the combination strategy of 2-3-4 and 6-7-8. It is possible to test all the cycles in all the 28 two-dimensional subspaces. We can also archive the discovery of the fine structure.

6.7.4 Related work on high dimension game dynamics pattern

- In natural science, there are many real examples. In ecology, game dynamics pattern, as rock-paper-scissors, has been seen in male lizard competing [9]. If a ecology have more spices take into account, higher dimension dynamics analysis technologies are needed.
- In economics, there are many practical examples, too [9].. In a financial markets system, or supply chain, or public goods providing and protecting, there are always many players and each player has many strategy. To describe such systems, high dimensional dynamics analysis technologies are needed too.
- In artificial intelligence study, this is also visible If the game is approximately transitive, then self-play generates sequences of agents of increasing strength. However, nontransitive games, such as rock-paper-scissors in poker or StarCraft [1][21][4]. can exhibit a dynamics structure (strategic cycles), and there is no longer a clear objective and against whom is unclear. In such game system, the dimension is extremely high, to test out the nontransitive strategy (component) is cruelly important.

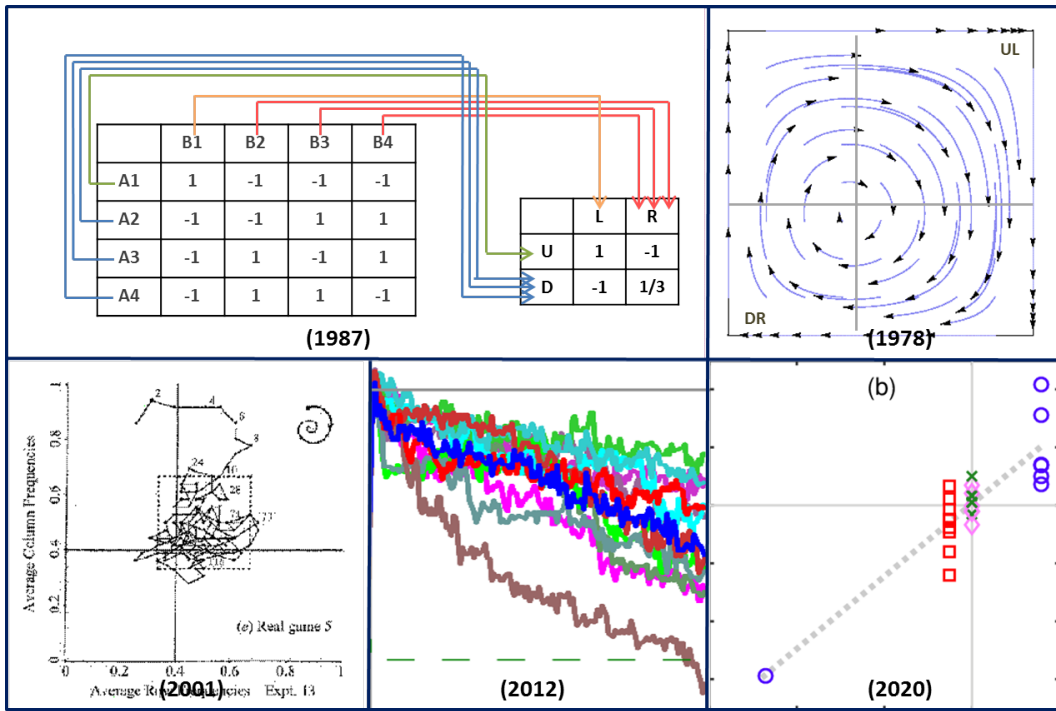


Figure 8: (1987) The O'Neill 4×4 original matrix and Binmore 2×2 concentration matrix. (1978) The replicator dynamics trajectory by Binmore's 2×2 concentration matrix. (2001) The figure (from [15]) with two-rounds average trajectory from a manual selection session, with unclear existence of a cycle in the long run. (2012) The figure (from [23]) reports the 150-round accumulated angular momentum of the 13 sessions in the two-dimensional presentation, with the accumulated angular momentum in abscissa and the experiment time (rounds) in ordinate dimension. (2020) The result from the eigencycle while exploring the eight-dimensional decomposed cycles, with theoretical eigencycle value σ in abscissa and experimental angular momentum L in ordinate dimension.